

Energetics of Formation and X-ray Crystal Structures of $\overline{\text{SNSNS}}(\text{MF}_6)_2$ ($\text{M} = \text{As}, \text{Sb}$), Containing the Lattice-Stabilized, Aromatic, 6π 1,3,4,2,5-Trithiadiazolium(2+) Cation Formed by the Crystal-Lattice-Enforced Symmetry-Allowed Cycloaddition of SN^+ and SNS^+

Wendell V. F. Brooks,^{*,†} T. Stanley Cameron,^{*,‡} Simon Parsons,[†] Jack Passmore,^{*,†} and Melbourne J. Schriver[†]

Departments of Chemistry, University of New Brunswick, Fredericton, New Brunswick, Canada E3B 6E2, and Dalhousie University, Halifax, Nova Scotia, Canada B3H 4J3

Received March 3, 1994[⊗]

$\overline{\text{SNSNS}}(\text{AsF}_6)_2$, formed by the lattice-enforced symmetry-allowed cycloaddition of SN^+ and SNS^+ , was obtained in quantitative yield by the evaporation of a solution of SNAsF_6 and SNSAsF_6 in SO_2 and characterized by vibrational spectroscopy and X-ray crystallography. Crystal data: space group $C2$ (No. 5), $a = 12.558(2)$ Å, $b = 8.454(1)$ Å, $c = 10.583(2)$ Å, $\beta = 92.51(2)^\circ$, $Z = 4$, $R = 3.98\%$ ($R_w = 4.71\%$) for 770 observed reflections and 163 independent parameters. Although it has long been predicted to be a stable, 6π , electron-rich aromatic, the $\overline{\text{SNSNS}}^{2+}$ cation dissociates reversibly in SO_2 solution (^{14}N NMR), but is stable in the solid state in $\overline{\text{SNSNS}}(\text{MF}_6)_2$ ($\text{M} = \text{As}, \text{Sb}$). This is consistent with the results of fully optimized $6\text{-}31\text{G}^*$ MO calculations, from which $\Delta H[\text{SN}^+(\text{g}) + \text{SNS}^+(\text{g}) \rightarrow \overline{\text{SNSNS}}^{2+}(\text{g})] = +400$ kJ mol⁻¹. However, in the solid state, the high lattice energy of $\overline{\text{SNSNS}}(\text{AsF}_6)_2$ (1493 kJ mol⁻¹) compared to the combined lattice energies of $\text{SNAsF}_6 + \text{SNSAsF}_6$ (1065 kJ mol⁻¹) stabilizes the 1:2 salt over the two 1:1 salts. In SO_2 solution simple thermochemical estimates suggest that $\text{SNS}^+(\text{SO}_2)$ and $\text{SN}^+(\text{SO}_2)$ are marginally more stable than $\overline{\text{SNSNS}}^{2+}(\text{SO}_2)$. This is consistent with the observed stability in SO_2 of the related selenium containing cations $\text{Se}_x\text{S}_{3-x}\text{N}_2^{2+}$ ($x = 1-3$), which results from the well-known preference of Se for σ -bonded structures. The similarity of $\text{Se}_x\text{S}_{3-x}\text{N}_2^{2+}$ cations is supported by a normal coordinate analysis of their vibrational spectra (for $x = 0, 2, 3$) which shows that a consistent set of force constants characterizes their force fields. The stability of salts of $\overline{\text{SNSNS}}^{2+}$ in the solid state depends critically upon the lattice energy, which is reduced in the presence of large counteranions. Consistently, while we were able to prepare $\overline{\text{SNSNS}}(\text{SbF}_6)_2$ (Raman, X-ray crystallography), an attempt to obtain $\overline{\text{SNSNS}}(\text{Sb}_2\text{F}_{11})_2$ gave only a mixture of $\text{SNS}(\text{Sb}_2\text{F}_{11})$ and $\text{SN}(\text{Sb}_2\text{F}_{11})$ (Raman). The structure of $\overline{\text{SNSNS}}(\text{SbF}_6)_2$ was determined by single crystal X-ray diffraction: monoclinic space group $P2_1/n$, $a = 12.928(3)$ Å, $b = 31.619(7)$ Å, $c = 8.778(5)$ Å, $\beta = 90.26(3)^\circ$, $V = 3588(2)$ Å³, $Z = 12$, which is a supercell of an orthorhombic $Pna2_1$ system ($a = 10.544(2)$ Å, $b = 12.952(3)$ Å, $c = 8.801(4)$ Å, $V = 1201.9(7)$ Å³, $Z = 4$). This supercell probably extends to a yet larger supercell which has not been examined.

Introduction

The $\overline{\text{SNSNS}}^{2+}$ heterocycle (**1**) has long been of interest in sulfur-nitrogen chemistry as an example of a 6π "electron-rich aromatic".¹ No conclusive evidence for this cation has yet been presented. Paradoxically, the 7π radical cation $\overline{\text{SNSNS}}^{\cdot+}$, present in $\text{S}_3\text{N}_2\text{Cl}_2$ discovered by Demarçay in 1880,² is indefinitely stable,³ although its structure has only been known since Banister's classic studies.^{3a} Roesky⁴ and Mews⁵ have

prepared compounds which analysed as $1(\text{SbCl}_6)_2$ and $1(\text{AsF}_6)_2$, although direct structural evidence was not presented. We recently prepared and characterized the series of cations $\text{Se}_x\text{S}_{3-x}\text{N}_2^{2+}$ ($x = 1-3$), and showed that they are indefinitely stable in the solid state and in solution.^{6-9a} We now describe the preparation and characterization of $1(\text{MF}_6)_2$ ($\text{M} = \text{As}, \text{Sb}$) by vibrational spectroscopy and X-ray crystallography and account for the formation of **1** by the lattice energy driven cycloaddition of SNS^+ and SN^+ on generation of the crystalline solid. Far from being a stable 6π species, **1** is only stable in

[†] University of New Brunswick.

[‡] Dalhousie University.

[⊗] Abstract published in *Advance ACS Abstracts*, November 1, 1994.

- (1) Chivers, T. *Acc. Chem. Res.* **1984**, *17*, 166. Chivers, T. *Chem. Rev.* **1985**, *85*, 341.
- (2) Heal, H. G. *The Inorganic Heterocyclic Chemistry of Sulfur, Nitrogen and Phosphorus*; Academic Press: London, 1980; see also references therein.
- (3) (a) Small, R. W. H.; Banister, A. J.; Hauptman, Z. V. *J. Chem. Soc., Dalton Trans.* **1984**, 1377. Banister, A. J.; Clarke, H. G. Rayment, I.; Shearer, H. M. M. *Inorg. Nucl. Chem. Lett.* **1974**, *10*, 647. (b) Gillespie, R. J.; Kent, J. P.; Sawyer, J. F. *Inorg. Chem.* **1981**, *20*, 3784. (c) Preston, K. F.; Charland, J.-P.; Sutcliffe, L. H. *Can. J. Chem.* **1988**, *66*, 1299.

(4) Roesky, H. W.; Dieltl, M. *Chem. Ber.* **1973**, *106*, 3101.

(5) Padma, D. K.; Mews, R. Z. *Naturforsch.* **1987**, *42B*, 699.

(6) Awere, E. G.; Passmore, J.; White, P. S.; Klapötke, T. *J. Chem. Soc., Chem. Commun.* **1989**, 1415.

(7) Awere, E. G.; Passmore, J.; White, P. S. *J. Chem. Soc., Dalton Trans.* **1992**, 1267. *Erratum: J. Chem. Soc., Dalton Trans.* **1992**, 2427.

(8) Awere, E. G.; Passmore, J.; White, P. S. *J. Chem. Soc., Dalton Trans.* **1993**, 299.

(9) (a) Awere, E. G. Ph.D. Thesis, Department of Chemistry, University of New Brunswick, Fredericton, NB, Canada, 1992. Awere, E. G.; Brooks, W. V. F.; Cameron, T. S.; Passmore, J.; White, P. S.; Sun, X. *J. Chem. Soc., Dalton Trans.* **1993**, 2439. (b) See refs 10a and 47 below.

the solid state, and quantitatively dissociates in SO₂ solution back to SN⁺ and SNS⁺. This is consistent with estimates of the solution energetics, and lattice energy and *ab initio* calculations, which show that although^{9b} $\Delta H[\text{S}_3\text{N}_2^{2+}(\text{g}) \rightarrow \text{SN}^+(\text{g}) + \text{SNS}^+(\text{g})]$ is -400 kJ mol^{-1} , **1** is stabilized in the solid state by the high lattice energy of the 1:2 salt. As such, we describe **1** as lattice stabilized, and the reaction of SN⁺ and SNS⁺ as being the first example of a "lattice-enforced" cycloaddition. A preliminary account of part of this work has been given.^{10a,b}

Experimental Section

Apparatus, techniques, and chemicals, unless specified, have been previously described.¹¹ SNAsF₆,¹² SNSAsF₆,^{13a} and FSNSNSAsF₆¹⁴ were prepared according to the literature procedures. SbF₅ (Ozark-Mahoning) was triply distilled prior to use. SO₂ (Matheson) was dried over CaH₂. All solids were manipulated under dry nitrogen in a Vacuum Atmospheres Dri-Lab. All apparatus was carefully dried prior to use.

NMR spectra were acquired on a Varian Associates XL-200 spectrometer, using previously described acquisition and referencing procedures.¹⁵ Samples were contained in thick-walled 10 mm precision NMR tubes (Wilmad) fitted with J Young O-Ringette type valves. Infrared spectra were obtained as Nujol mulls between KBr (4000–350 cm⁻¹) or CsI (4000–200 cm⁻¹) plates on a Perkin-Elmer 683 instrument. Raman spectra of samples contained in sealed melting point tubes or thin-walled 5 mm NMR tubes were obtained at room temperature on a Spex Ramalab instrument using a green line laser (Ar, $\lambda = 5145 \text{ \AA}$) and a slit width of 4 and/or 8 cm⁻¹. FT-Raman spectra were obtained on a Bruker IFS-66 FT-IR spectrometer outfitted with an FRA-106 FT-Raman accessory. The incident laser beam was defocused in order to prevent sample-heating, and the scattered radiation was collected in the 180° backscattering mode. The data were treated with a Norton–Beer (medium) apodization function,^{16,17} and spectra were obtained with a resolution of 2 cm⁻¹.

Elemental analyses were carried out by Beller Mikroanalytisches Laboratorium, Göttingen, Germany.

Preparation and Crystal Growth of 1(AsF₆)₂. SO₂ (4.490 g) was condensed onto SNAsF₆ (0.444 g, 1.89 mmol) and SNSAsF₆ (0.479 g, 1.79 mmol) in one bulb connected via a Rotoflo valve and a medium porosity glass frit to a second bulb; the whole vessel was closed with another Rotoflo valve. The clear yellow solution was stirred for 2 days at 25 °C with no change in appearance. The solution was cooled to 3 ± 2 °C in a cold room, and the solvent removed over the course of 3 weeks by cooling the second bulb to 0 °C in an ice/water mixture, giving clear yellowish crystals, which were quickly washed with a little SO₂, filtered, and then isolated by closing the first valve and cooled to -20 °C. The volatiles were then removed at 25 °C under dynamic vacuum, leaving a pale yellow residue. The crystals were subjected to dynamic vacuum at -20 °C just until their surfaces began to acquire a powdery appearance (15 s), giving a very pale yellow solid lump (0.645 g, 70% yield), which contained a large number of crystals. The total mass of the solid products after removal of the volatiles was 0.960

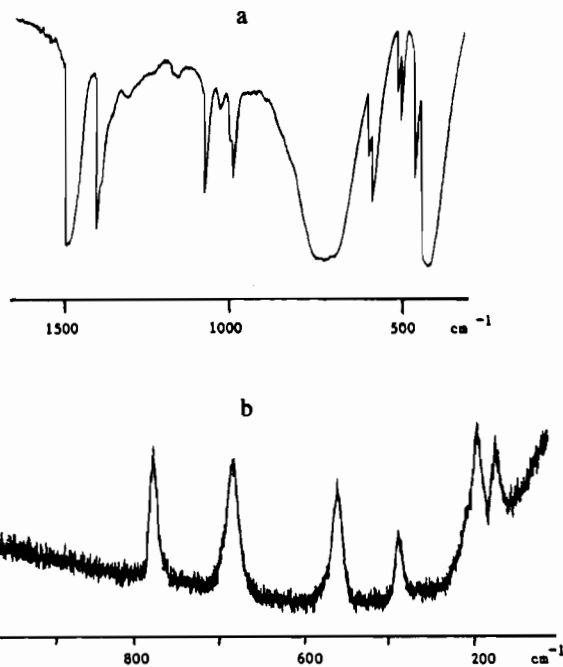


Figure 1. (a) Infrared spectrum of **1**(AsF₆)₂ as a Nujol mull between KBr plates. (b) Raman spectrum of **1**(AsF₆)₂.

g (cf. calculated 0.920 g). Several crystals were quickly picked and loaded into rigorously dried glass capillaries, taken to Dalhousie University packed in dry ice, and identified as **1**(AsF₆)₂ by X-ray crystallography. A sample of **1**(AsF₆)₂ acquired a prominent red surface coloration when stored at -20 °C under dry nitrogen for 5 months.

In situ ¹⁴N NMR Study of the Reaction between SNSAsF₆ and SNAsF₆ and Infrared and Raman Spectra of 1(AsF₆)₂. SO₂ (1.79 g) was condensed onto a mixture of SNAsF₆ (0.267 g, 1.0 mmol) and SNSAsF₆ (0.263 g, 1.12 mmol) in a 10 mm NMR tube. The solution became opaque green-black on warming to room temperature, but was clear yellow after 20 min. After one h the ¹⁴N NMR spectrum showed two resonances at -91 ppm (SNS⁺, $\Delta\nu = 8 \text{ Hz}$) and 202 ppm (SN⁺, $\Delta\nu = 250 \text{ Hz}$) with approximately equal integrations.^{10b} The spectrum was unchanged at -20 °C, although cooling the solution below this temperature caused a white solid to precipitate. The solvent was removed over four h at -20 °C, leaving a white solid, which was characterized by its Raman (*in situ*) and infrared spectra (Nujol mull; see Figure 1 and Table 1). The Raman spectrum only exhibited bands assignable to **1**(AsF₆)₂, but the IR spectrum showed several additional bands due to FSNSNSAsF₆, as well as a very weak band at 1490 cm⁻¹ assignable to excess SNSAsF₆¹⁸ (not included in Table 1). Neither spectrum showed bands due to SNAsF₆. The white solid was redissolved in SO₂ (2 g), giving a yellow solution, the ¹⁴N NMR spectrum of which was identical to that described above. Removal of the volatiles gave a tan solid which was heated to 80 °C under dynamic vacuum for 20 h, giving a brown solid, the IR of which, though similar to that described above, showed in addition much stronger bands due

to FSNSNSAsF₆.^{5,14} ¹⁴N NMR in SO₂ (2 g): -170 and -30 ppm (FSNSNS⁺, broad, 20% of total integration), -91 ppm (SNS⁺, $\Delta\nu = 8 \text{ Hz}$, 40%), 200 ppm (SN⁺, $\Delta\nu = 300 \text{ Hz}$, 40%).^{10b,14}

Preparation of 1(AsF₆)₂ by the Reaction of FSNSNSAsF₆ with AsF₅. SO₂ (3.59 g) and AsF₅ (0.248 g, 1.46 mmol) were condensed onto FSNSNSAsF₆ (0.326 g, 0.98 mmol) in a 10 mm NMR tube, giving a very dark red solution, which became pale yellow over 20 h. The ¹⁴N NMR spectrum contained two resonances due to equimolar amounts of SNS⁺ and SN⁺, and slow removal of the volatiles gave a brown solid identified by IR as **1**(AsF₆)₂ contaminated with FSNSNSAsF₆.

- (10) (a) Brooks, W. V. F.; Cameron, T. S.; Grein, F.; Parsons, S.; Passmore, J.; Schriver, M. J. *J. Chem. Soc., Chem. Commun.* **1991**, 1079. (b) Passmore, J.; Schriver, M. J. *Inorg. Chem.* **1988**, *27*, 2749.
- (11) Passmore, J.; Taylor, P. J. *Chem. Soc., Dalton Trans.* **1976**, 804. Passmore, J.; Richardson, E. K.; Taylor, P. *Inorg. Chem.* **1978**, *17*, 1681. Desjardins, C. D.; Passmore, J. *J. Fluorine Chem.* **1975**, *6*, 379. Lau, C.; Passmore, J. *J. Chem. Soc., Dalton Trans.* **1973**, 2528. Murchie, M. P.; Passmore, J. *Inorg. Synth.* **1986**, *24*, 76.
- (12) Apbiett, A.; Banister, A. J.; Biron, D.; Kendrick, A. G.; Passmore, J.; Schriver, M.; Stojanac, M. *Inorg. Chem.* **1986**, *25*, 4451.
- (13) (a) Awere, E. G.; Passmore, J. *J. Chem. Soc., Dalton Trans.* **1992**, 1343. Banister, A. J.; Hey, R. G.; Maclean, G. K.; Passmore, J. *Inorg. Chem.* **1982**, *21*, 1679. (b) Bonnet, B.; Mascherpa, G. *Inorg. Chem.* **1980**, *19*, 785. Gillespie, R. J.; Landa, B. *Inorg. Chem.* **1973**, *12*, 1383.
- (14) Parsons, S.; Passmore, J.; Schriver, M. J.; Sun, X. *Inorg. Chem.* **1991**, *30*, 3342 and references therein. See also ref 5.
- (15) Parsons, S.; Passmore, J.; Schriver, M. J.; White, P. S. *Can. J. Chem.* **1989**, *68*, 852.
- (16) Norton, R. H.; Beer, R. *J. Opt. Soc. Am.* **1976**, *66*, 259.
- (17) Norton, R. H.; Beer, R. *J. Opt. Soc. Am.* **1977**, *67*, 419.

- (18) No excess SNSAsF₆ was observed in the Raman spectrum, although it was observed in the IR spectrum. IR spectra are likely more representative of the whole sample than the Raman spectra, which are taken at one point in the sample. It is likely that the excess SNSAsF₆ was precipitated first and was at the very bottom of the tube.

Table 1. Vibrational Data for the $\overline{\text{SNSNS}}^{2+}$ Cation (1)

$1(\text{AsF}_6)_2$		$1(\text{SbF}_6)_2^a$	
IR	Raman	FT-Raman	assign
1051 (s)	1060 (w)	1056 (w)	$\nu_1(\mathbf{1})^b$
1012 (w)			$\text{S}_3\text{N}_2\text{F}^+$
980 (sh)			$\text{S}_3\text{N}_2\text{F}^+$
968 (m)	972 (vw)	972 (vw)	$\nu_3(\mathbf{1})$
	780 (s)	777 (vs)	$\nu_2(\mathbf{1})$
699 (vs)	696 (sh)		$\nu_3(\text{AsF}_6^-)$
	688 (s)	680 (mw)	$\nu_1(\text{AsF}_6^-)$
668 (sh)			$\nu_6(\mathbf{1})$
		653 (vs)	$\nu_1(\text{SbF}_6^-)$
573 (m, sh)	575 (sh)		$\text{S}_3\text{N}_2\text{F}^+(\text{IR})$
		570 (sh)	$\nu_2(\text{SbF}_6^-)$
558 (s)	562 (s)	555 (s)	$\nu_2(\text{AsF}_6^-)$
497 (m, sh)			$\text{S}_3\text{N}_2\text{F}^+$
483 (ms)	490 (m)	490 (m)	$\nu_3(\mathbf{1})$
438 (m)			$\nu_7(\mathbf{1})$
	395 (s)	405 (vs)	$\nu_4(\mathbf{1})$
388 (vs)			$\nu_4(\text{AsF}_6^-)$
	372 (ms)	373 (w)	$\nu_5(\text{AsF}_6^-)$
		286 (w)	$\nu_5(\text{SbF}_6^-)$

^a Actual spectrum is deposited in the supplementary material. Four similar laser Raman spectra were also obtained. ^b See Table 4 for descriptions of $\text{S}_3\text{N}_2^{2+}$ vibrations.

Preparation of $1(\text{SbF}_6)_2$. SNAsF_6 (0.481 g, 2.05 mmol) and SNSAsF_6 (0.532 g, 1.99 mmol) were dissolved in SO_2 (4.041 g) in one bulb of a two-bulbed vessel, similar to that described above, and poured onto SbF_5 (0.958 g, 4.37 mmol) contained in the second bulb. The solution was initially light green, but became yellow after 10 min at room temperature. The solution was stirred for 3 days at 25 °C with no further color changes. The solvent was slowly (12 h) condensed back into the second over 12 h leaving a white crystalline solid (1.428 g), which was quickly washed with a little SO_2 . Most of the reaction volatiles were condensed into a 10 mm NMR tube and identified as SO_2 and AsF_5 (^{19}F NMR); the remaining volatiles (probably including excess SbF_5) were removed under dynamic vacuum. Large, colorless crystals were grown by slow evaporation of a solution of the solid in fresh SO_2 (5.849 g) at room temperature. The Raman spectrum of the solid (Table 1 and supplementary material) was consistent with $1(\text{SbF}_6)_2$, although an additional band at 682 cm^{-1} is attributable to residual AsF_6^- ($\nu_1(\text{AsF}_6^-)$, 688 cm^{-1}). Anal. Calcd for $1(\text{SbF}_6)_2$: N, 4.70; S, 16.14; F, 38.27. Found: N, 4.75; S, 16.61; F, 40.9. There was no change in the appearance or Raman spectrum of a sample of crystalline $1(\text{SbF}_6)_2$ stored under dry nitrogen at -20 °C for 1 year.

Attempted Preparation of $1(\text{Sb}_2\text{F}_{11})_2$. Following a similar procedure to that described above, a solution of SNAsF_6 (0.371 g, 1.58 mmol) and SNSAsF_6 (0.401 g, 1.50 mmol) in SO_2 (4.854 g) was poured onto SbF_5 (1.3589 g, 6.3 mmol), giving a yellow solution which was stirred at 25 °C for 15 h. Slow removal (overnight) of the volatiles under dynamic vacuum at room temperature led only to a yellow orange oil (2.367 g). An FT-Raman spectrum of the oil (which is provided with assignments in the supplementary material) showed only bands assignable to SN^+ ,¹² SNS^+ ,^{13a} and $\text{Sb}_2\text{F}_{11}^-$.^{13b}

Crystal Structure of $1(\text{AsF}_6)_2$. Intensity data were collected on a CAD4 four-circle diffractometer with an ω -2 θ scan. The data were reduced¹⁹ to a standard scale; Lp and absorption corrections were applied.²⁰ The positions of the As and S atoms were derived from an E-map (SHELXS),²¹ and the positions of the remaining F and N atoms were determined from subsequent Fourier syntheses. The structure was refined, initially using large-block least-squares (SHELX76)²² and

Table 2. Crystal Data

	$1(\text{AsF}_6)_2$	$1(\text{SbF}_6)_2$
crystal system	monoclinic	monoclinic
space group	C2	$P2_1/n$
<i>a</i> , Å	12.558(2)	12.928(3.0)
<i>b</i> , Å	8.454(1)	31.619(6.0)
<i>c</i> , Å	10.583(3)	8.778(4.0)
β , deg	92.51(2)	90.26(2.0)
<i>V</i> , Å ³	1122.5(3)	3588.2(7)
<i>Z</i>	4	12
<i>fw</i>	502.017	1786.72 = 3 × 595.57
crystal dimens., mm	0.15 × 0.22 × 0.28	0.10 × 0.15 × 0.23
<i>F</i> (000)	944	3264
<i>D_x</i> , Mg m ⁻³	2.970	3.3072
abs coeff, cm ⁻¹	66.24	51.88
diffractometer	CAD4	AFC5R
radiation	Mo K α (sealed tube)	Mo K α (rotating anode)
no. of measd reflns	952	4109
no. of unique reflns	897	3885
no. of reflns (<i>I</i> > 3 σ (<i>I</i>))	770	2269
no. of params	163	424 (SbF ₆ ⁻ as restrained rigid bodies)
<i>R</i> ^a	0.0398	0.065
<i>R_w</i> ^b	0.0471	0.065
weighting scheme used	$w = 1.049/(\sigma^2(F) + 0.123(F^2))$	unit weights

$$^a R = \sum(|F_o| - |F_c|)/\sum|F_o|. \quad ^b R_w = [(\sum w(|F_o| - |F_c|)^2)/\sum w F_o^2]^{1/2}.$$

subsequently with full-matrix least-squares (CRYSTALS).²³ The refinement converged with *R*=3.89% with anisotropic temperature factors on all atoms. The structure is in space group C2 where the origin along *y* is not fixed by symmetry. In the final stages of the refinement the origin was fixed by requiring the sum of all *y* shifts to equal zero. The enantiomer was checked by refining the structure in both possible "hands" and the parameters reported here gave a drop in *R* of 1.4% when *R* had stood at 5.2%. There are three unique As atoms in the structure, one belonging to an AsF_6^- anion, the other two As atoms are on 2-fold axes, thus contributing half an AsF_6^- anion each. While the anisotropic vibrations of the fluorine atoms of the three AsF_6^-

are larger than those of the $\overline{\text{SNSNS}}^{2+}$ ring, they are not unreasonably large and present (for this anion) a remarkably unordered picture.

Crystal data and final atomic coordinates are given in Tables 2 and 3a, respectively. Anisotropic thermal parameters and full details of the structure determination and the refinement have been deposited as supplementary material.

Crystal Structure of $1(\text{SbF}_6)_2$. A colorless prismatic crystal was mounted in a glass capillary under dry nitrogen. All measurements were made on a Rigaku AFC5R diffractometer with a graphite monochromated Mo K α radiation and an RU200 12 kW rotating anode generator. Cell constants and orientation matrix for data collection, obtained from a least-squares refinement using setting angles $43.11 < 2\theta < 48.78^\circ$ corresponded initially to an orthorhombic cell with dimensions *a* = 10.544(2), *b* = 12.952(3), and *c* = 8.801(4) Å, *V* = 1201.9(7) Å³, *Z* = 4, and *M* = 595.57 and 880 reflections with *I* > 3 σ (*I*).²⁴ Based on systematic absences of *Ok**l* (*k* + *l* ≠ 2*n* + 1) and *h*0*l* (*h* ≠ 2*n* + 1), the cell angles which did not differ significantly from 90° (α = 90.234(72), β = 90.059(25), γ = 90.018(17)°), Laue symmetry not inconsistent with *mm*2, the intensity statistics and the subsequent refinement, a possible space group is *Pna*2₁. The structure refined with seriously disordered $\text{S}_3\text{N}_2^{2+}$ and SbF_6^- groups and, depending upon the degree of the disorder, the *R* factor could be reduced to a value somewhere about 0.10. The structure could also be refined in a disordered monoclinic cell *P*2₁ but here there were very severe parameter correlations.

(19) Cameron, T. S.; Cordes, R. E. *Acta Crystallogr.* **1979**, *35B*, 748.

(20) Walker, N.; Stuart, D. *Acta Crystallogr.* **1983**, *39A*, 158.

(21) Sheldrick, G. M. In *Crystallographic Computing 3*; Sheldrick, G. M., Kruger, C., Goddard, R., Eds.; Oxford University Press: Oxford, England, 1985; pp 175–189.

(22) Sheldrick, G. M. SHELX: A system of computer programs for X-ray structure determination, as locally implemented at Dalhousie University and Cambridge University, 1975.

(23) Curruthers, J. R.; Watkin, D. J. *CRYSTALS (Issue 8)*; Chemical Crystallography Laboratory: Oxford, England, 1989.

(24) The crystal structure of $\overline{\text{SeNSNS}}(\text{AsF}_6)_2^{9a}$ (but not $\overline{\text{SeNSeNSe}}(\text{AsF}_6)_2^8$ or $\overline{\text{SeNSNSe}}(\text{AsF}_6)_2^7$) shows a similar feature, and these may be two examples of a polytypical family.

Table 3. Fractional Atomic Positional and Equivalent Isotropic Temperature Factors with Esd's in Parentheses

atom	<i>x/a</i>	<i>y/b</i>	<i>z/c</i>	<i>U</i> (iso), ^a Å ²	atom	<i>x/a</i>	<i>y/b</i>	<i>z/c</i>	<i>U</i> (iso), ^a Å ²
(a) 1(AsF ₆) ₂									
S(1)	1461(2)	6720(3)	2559(2)	391	F(15)	7476(8)	7382(12)	2491(14)	933
S(2)	2049(2)	9541(4)	1528(3)	436	F(16)	9163(10)	7324(16)	1400(10)	958
S(3)	2115(3)	9592(4)	3507(3)	459	As(2)	0	3308	5000	362
N(1)	1654(8)	7828(13)	1369(9)	444	F(21)	799(8)	4740(10)	4416(10)	681
N(2)	1757(7)	7887(13)	3692(8)	353	F(22)	780(8)	1890(11)	4387(10)	720
As(1)	8645.8(6)	8479(2)	2508.8(9)	363	F(23)	-786(7)	3355(17)	3658(9)	853
F(11)	8072(6)	9647(13)	1398(7)	643	As(3)	0	3255	0	348
F(12)	9171(8)	7266(15)	3613(10)	877	F(31)	609(9)	4634(13)	916(12)	826
F(13)	9776(6)	9556(13)	2564(10)	765	F(32)	-1065(7)	3205(17)	926(10)	905
F(14)	8093(7)	9622(14)	3624(7)	712	F(33)	582(10)	1871(13)	901(13)	897
(b) 1(SbF ₆) ₂									
Sb(1)	2617(3)	166(1)	7281(4)	229(11)	F(21)	4581(12)	612(10)	3661(13)	622(21)
Sb(2)	7630(4)	1498(2)	2428(5)	442(15)	F(22)	3185(12)	1145(11)	792(13)	1182(22)
Sb(3)	2372(2)	1828(1)	7256(3)	121(11)	F(23)	2811(12)	690(10)	3060(13)	835(30)
Sb(4)	3914(3)	894(2)	2310(4)	376(12)	F(24)	5095(13)	1092(11)	1452(13)	1023(15)
Sb(5)	8893(4)	773(2)	7676(5)	591(12)	F(25)	7726(13)	1031(12)	7107(13)	670(22)
Sb(6)	6090(4)	2445(2)	7418(6)	641(13)	F(26)	10040(13)	578(12)	8496(13)	880(16)
S(1)	4607(8)	2185(3)	3377(8)	227(14)	F(27)	9125(13)	1258(11)	8801(13)	422(23)
S(2)	4301(9)	2820(3)	3813(9)	409(13)	F(28)	8803(13)	356(12)	6387(13)	814(18)
S(3)	4030(7)	2615(3)	819(9)	158(20)	F(29)	9621(13)	1003(12)	6283(13)	408(16)
S(4)	698(10)	1161(5)	3767(10)	727(22)	F(30)	8247(13)	522(11)	9118(13)	308(15)
S(5)	443(10)	519(5)	3401(9)	739(14)	F(31)	5100(13)	2129(11)	8339(13)	619(24)
S(6)	966(8)	963(4)	814(10)	325(16)	F(32)	7180(13)	2702(12)	7145(13)	790(16)
S(7)	5441(9)	1153(3)	8342(8)	370(15)	F(33)	6548(13)	1978(12)	6434(13)	947(26)
S(8)	5843(11)	527(4)	8773(10)	942(14)	F(34)	5723(13)	2859(12)	8766(13)	712(19)
S(9)	5949(10)	716(5)	5849(10)	797(20)	F(35)	5211(13)	2626(11)	6054(13)	369(15)
F(1)	3770(12)	521(10)	7308(13)	753(20)	F(36)	7073(13)	2224(11)	8973(13)	612(24)
F(2)	1426(13)	-219(11)	7233(13)	838(15)	F(111)	4927(13)	2300(12)	6369(13)	642(14)
F(3)	2097(13)	433(11)	9016(13)	967(14)	F(112)	7257(13)	2581(13)	8424(14)	1334(14)
F(4)	3112(12)	-108(9)	5600(13)	585(14)	F(113)	5754(13)	2072(12)	8871(13)	812(14)
F(5)	1926(12)	551(8)	6069(13)	659(17)	F(114)	6406(13)	2827(13)	5947(14)	1297(15)
F(6)	3363(12)	-205(9)	8566(13)	568(16)	F(115)	5390(13)	2847(12)	8435(13)	731(15)
F(7)	6999(13)	1117(10)	3681(13)	874(15)	F(116)	6787(13)	2033(13)	6383(14)	1560(14)
F(8)	8377(12)	1900(10)	1428(13)	869(18)	F(211)	9282(13)	1230(11)	8798(13)	530(14)
F(9)	6493(12)	1863(9)	2720(13)	552(16)	F(212)	8528(13)	325(12)	6526(13)	1030(14)
F(10)	8716(13)	1131(9)	2232(13)	916(18)	F(213)	7811(13)	1069(12)	6898(13)	633(27)
F(11)	6948(12)	1284(9)	796(13)	600(14)	F(214)	9977(13)	479(12)	8438(13)	790(15)
F(12)	8260(13)	1698(10)	4168(13)	946(15)	F(215)	8095(13)	582(12)	9210(13)	999(15)
F(13)	1775(13)	1519(10)	5745(13)	969(14)	F(216)	9707(13)	963(13)	6142(13)	987(14)
F(14)	2977(12)	2165(9)	8659(13)	664(16)	N(1)	4022(12)	2948(4)	2191(8)	361(13)
F(15)	1644(13)	1545(9)	8735(13)	909(15)	N(2)	4286(12)	2187(4)	1694(8)	380(15)
F(16)	3076(12)	2097(9)	5683(13)	577(15)	N(3)	571(12)	546(4)	1644(9)	188(14)
F(17)	1279(12)	2185(8)	7113(13)	483(15)	N(4)	1099(12)	1288(5)	2184(9)	682(14)
F(18)	3430(13)	1451(9)	7467(13)	694(15)	N(5)	6094(12)	376(6)	7170(9)	621(14)
F(19)	3786(13)	1346(12)	3507(13)	1809(14)	N(6)	5556(12)	1142(5)	6612(8)	223(27)
F(20)	4158(13)	460(11)	1004(13)	1113(16)					

^a *U*(iso) is one-third of the trace of the thermal ellipsoid tensor.

There was however a set of additional, sharply-defined but weak reflections. When unit cell dimensions were determined using 25 of the strongest of these reflections, the cell was found to be consistent with a larger monoclinic cell of dimensions $a = 12.928(3)$, $b = 31.619(7)$, and $c = 8.778(5)$ Å, $\beta = 90.26(3)^\circ$, $V = 3588(2)$ Å³, $Z = 12$ (3×4), and $M = 1786.72$ ($= 3 \times 595.57$). These additional weak reflection increased the total number of reflections with $I > 3\sigma(I)$ from 1760 (2×880) to 2269, an additional 509 reflections. Based on systematic absences of $h0l$ ($h + l \neq 2n + 1$) and $0k0$ ($k \neq 2n + 1$), the intensity statistics which showed hypercentricity, and the subsequent refinement, the space group is $P2_1/n$.²⁵ The structure now refined with a converged R factor of 0.065, with only a little disorder in just two of the three unique $S_3N_2^{2+}$ groups and with four of the unique six SbF_6^- groups also without major disorder. The two remaining SbF_6^- groups showed signs of disorder in the positions of the fluorine atoms. Those attached to Sb(5) showed two sets of alternative positions separated from each other by a mean distance of 0.28(1) Å, while those attached to Sb(6) were in two completely different orientations. The crystal data and atomic coordinates are given in Tables 2 and 3b. A table of anisotropic thermal parameters, an extended table of crystal data, and a table of bond distances and angles have been deposited as supplementary material. This supercell corresponds to a tripling of the 10.544 Å axis of the smaller cell which becomes cell axis b in Figure 5 below. When

Figure 5 is examined, it can be seen that if b is reduced back to the small cell, the overlap of $S_3N_2^{2+}$ and SbF_6^- groups will give the $mm2$ symmetry which is observed in this smaller cell. Presumably the appropriate space group for the small cell is $P2_1$ with the 10.544 Å axis as the unique axis.

In addition to the tripling of the 10.544 Å axis, there is yet another set of even fainter reflections which correspond to a doubling of the 12.928 Å axis which introduce 32 more reflections with $I > 3\sigma(I)$. These now require that the space group be either $P2_1/c$ or $P\bar{1}$. It seems probable that a structure solution which took these reflections into account would resolve the major disorder of the $Sb(6)F_6^-$ groups, but

(25) When the supercell (Figure 5) is examined and reduced back to the subcell by dividing axis b by 3 and superimposing the sections, then the superimposition of the SbF_6^- and $S_3N_2^{2+}$ groups will give nearly $mm2$ symmetry. This is observed by the diffractometer software and since the beta angle is very close to 90° then the diffractometer software assumes an orthorhombic cell. The structure can be solved in this "orthorhombic" cell and can be refined to quite a reasonable R factor with (of course) severe disorder in both the anions and cations. Once the supercell structure has been resolved, it is clear the subcell has to be in a monoclinic space group. The most reasonable space group is probably $P2_1$, but given all the pseudo-symmetry there is little chance of producing any convincing refinement in this space group.

attempts to resolve this structure (now with a minimum of six $S_3N_2^{2+}$ and twelve SbF_6^- "unique" groups) were not successful. In view of this additional complication, the anisotropic thermal parameters for $1(SbF_6)_2$ should be viewed with caution.

Normal Coordinate Analyses. Vibrational analyses²⁶ of the three species $SNSNS^{2+}$, $SeNSNSe^{2+}$,⁷ and $SeNSeNSe^{2+}$ ^{6,8} were performed with the aim of seeing if the properties (especially the instability of **1** in solution and the gas phase (see below)) were correlated with the stretching force constants. Although we also have data on $SeNSNS^{2+}$,^{9a} more than seven force constants are required, and the crystal structure is disordered so that the distances are not well determined; the force constants are therefore not as well determined as for the other species, and are not included here. Our treatment deals only with the in-plane vibrations, ignores all crystal or ion-solvent forces, and assumes a simple valency force field with, at most, one interaction constant. Some of the seven in-plane frequencies can be identified by inspection of the spectra, but there are a number of debatable assignments; the selection rules do not help since all frequencies are both Raman and infrared active. The *ab initio* calculations of Grein²⁷ give frequencies that correspond well with observations for **1** (Table 4). Therefore we assigned the highest frequency, as predicted, to A, and similar assignments lead to good force constants for the other two species. We looked for economical force constant sets (six diagonal plus one off diagonal term) that give a good fit to the observed frequencies and correspond well with bond orders, as estimated from bond lengths.

Since the observed frequencies do not determine a unique set of force constants, we used Badger's rule²⁸ to give the ratio of force constants in a particular species (e.g. the constants of S-N bonds at the top [NSN] and sides [NSSN] of $SNSNS^{2+}$; see Table 4). Once a reasonable set of constants was found for $SNSNS^{2+}$ and $SeNSeNSe^{2+}$, the Badger's rule restriction was relaxed to obtain three stretching constants, three bending constants and one interaction constant (between the two N-S, or N-Se, bonds at the apex). Then initial force constants for $SeNSNS^{2+}$ were estimated which led to a solution. The complete final sets of force constants are included in the supplemental data. The force constants reproduce the observed frequencies to within less than 10 cm^{-1} (Table 4).

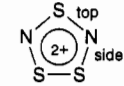
Our model for these ions is too simple to describe adequately the resonance interactions, the effects of ring strain and interactions with neighbouring ions or molecules. The higher (mostly stretching) modes are probably the least affected by these other forces and the stretching force constants give some useful insight into bond strengths. The bending constants are less consistent and more sensitive to changes in structure; at this point we feel they are not well enough determined to have any physical meaning.

Lattice Energy Calculations.²⁹ The lattice energy, U , of an ionic solid is given by³⁰

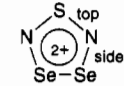
$$U = U_{elec} + U_{dd} + U_{dq} - U_r - U_z$$

where U_{elec} is the electrostatic energy of the lattice, U_{dd} is the dipole-induced dipole energy, U_{dq} is the dipole-induced quadrupole energy, U_r is the closed shell repulsion (or Born) term, and U_z is the zero point energy. Inclusion of a heat capacity term ($\int C_p dT$) gives the lattice enthalpy at 298 K. Calculation of these parameters has been discussed by Bartlett, and the reader is referred to ref 29 for full details. Lattice energies were obtained for $SNSbF_6$ (541.3 $kJ mol^{-1}$), $SNSAsF_6$ (509.4


Table 4. Observed and Calculated Fundamental Vibrational Frequencies and Calculated Potential Energy Distributions



obs	calc <i>ab initio</i> ^b	calc from force consts	class	potential energy distribn, % ^a			
				S-N top	S-N side	S-S	bend
1051	1077	1054	A ₁	40	50		
968	937	965	B ₂	25	75		35
780	791	776	A ₁	35	25		20
668	627	670	B ₂	55	20		35
483	580	484	A ₁	15	15	30	60
438	507	440	B ₂	40			45
395	409	395	A ₁			50	



obs ^c	calc from force consts	class	potential energy distribn, % ^a			
			S-N top	Se-N side	Se-Se	bend
970	967	A ₁	30	50		10
885	887	B ₂	40	55		
645	648	A ₁	35	25		30
500	497	B ₂	45	40		15
310	310	A ₁			85	15
290	291	B ₂				95
267	274	A ₁		25		70



obs ^d	calc from force consts	class	potential energy distribn, % ^a			
			Se-N top	Se-N side	Se-Se	bend
908	907	A ₁	60	30		
830	830	B ₂	55	40		
619	624	A ₁	20	40		40
520	518	B ₂	30	60		10
325	325	A ₁			85	10
276	275	B ₂	15			85
249	244	A ₁		30		60

^a Rounded to nearest 5% and minor contributions (<10%) not shown. ^b Reference 27. ^c Reference 7. ^d References 6 and 8.

$kJ mol^{-1}$) and $1(AsF_6)_2$ (1493.2 $kJ mol^{-1}$), and all relevant data are given in the supplementary material.

Since the crystal structure of $SNAsF_6$ has not been determined, its lattice energy could not be determined from an extended calculation of this type. Instead $U[SNAsF_6]$ was estimated using the linear correlation of U with $V^{-1/3}$ (V = estimated molar volume of AB in the unit cell) for AB salts developed by Bartlett:^{29,31}

$$U = 2336.5V^{-1/3} + 110.5 \quad (\text{in } kJ mol^{-1}; V \text{ in } \text{\AA}^3)$$

The volume of AsF_6^- is generally found to be ca. 10 \AA^3 less than that of SbF_6^- ,³² and so the molar volume of $SNAsF_6$ was estimated from that of $SNSbF_6$ ³³ to be 143 \AA^3 , giving a lattice energy of 556 $kJ mol^{-1}$. The lattice energy of $SNSbF_6$ calculated by this equation was 547 $kJ mol^{-1}$, in good agreement with 541 $kJ mol^{-1}$ obtained from the extended calculation.

- (26) Wilson, E. B., Jr.; Decius, J. C.; Cross, P. C. *Molecular Vibrations*; McGraw-Hill: New York, 1955.
 (27) Grein, F. (6-31G*, optimized geometry)⁴⁷ and personal communication.
 (28) (a) Badger, R. M. *J. Chem. Phys.* **1934**, *2*, 128. (b) Pauling, L. *The Nature of the Chemical Bond*, 3rd ed.; Cornell University Press: Ithaca, NY, 1960.
 (29) Mallouk, T. E.; Rosenthal, G. L.; Müller, G.; Brusasco, R.; Bartlett, N. *Inorg. Chem.* **1984**, *23*, 3167.
 (30) Dasent, W. E. *Inorganic Energetics*, 2nd ed.; Cambridge University Press: Cambridge, England, 1982.

- (31) Bartlett, N.; Yeh, S.; Kourtakis, K.; Mallouk, T. *J. Fluorine Chem.* **1984**, *26*, 97.
 (32) Penneman, R. A. *Inorg. Chem.* **1967**, *6*, 431.
 (33) Clegg, W.; Glemser, O.; Harms, K.; Hartmann, G.; Mews, R.; Noltemeyer, M.; Sheldrick, G. M. *Acta Crystallogr.* **1981**, *37B*, 548.

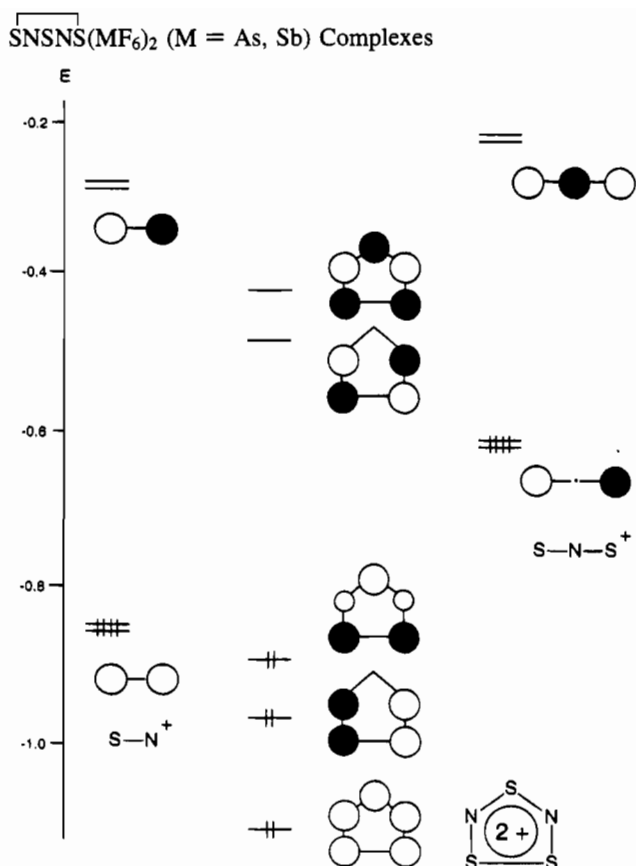
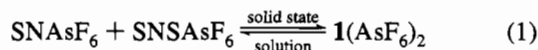


Figure 2. Orbital interactions during the cycloaddition of SNS^+ and SN^+ to give **1**, and the electronic structure of **1** ($6\text{-}31\text{G}^{**}/6\text{-}31\text{G}^*$).⁴⁷ The energy scale is relative and is in atomic units. The circles qualitatively represent the relative contribution of the atomic orbital to the corresponding π type molecular orbital. The LUMO of **1** becomes the SOMO of SNSNS^+ on formal one-electron reduction.

Results and Discussion

Preparation and Properties of $1(\text{AsF}_6)_2$. We previously showed^{14,34} that SNS^+ undergoes completely general, quantitative, reverse electron demand cycloadditions with alkynes and nitriles. The frontier molecular orbitals of SN^+ are isolobal with those of alkynes and nitriles, but much lower in energy (Figure 2; see also ref 35). A cycloaddition between SN^+ and SNS^+ to give **1** is therefore symmetry allowed, but the dominant orbital interaction is $\{\text{HOMO}(\text{SNS}^+) - \text{LUMO}(\text{SN}^+)\}$, making this the first cycloaddition involving SNS^+ to follow the normal electron demand regime.

A sample of crystalline $1(\text{AsF}_6)_2$ was prepared by the slow evaporation of a solution of SNAsF_6 and SNSAsF_6 in SO_2 at 3 ± 2 °C. A 5% excess of SNAsF_6 was used to convert traces of S_8 (usually present in very small amounts in SNSAsF_6 unless it is very highly purified) into SNSAsF_6 and then to $1(\text{AsF}_6)_2$. The product was kept at 3 ± 2 °C during crystal growth and the last traces of solvent removed at -20 °C to minimize the formation of FSNSNSAsF_6 . The total weight of the solid obtained from this reaction was only 40 mg more than expected on the basis of eq 1, consistent with the formation of $1(\text{AsF}_6)_2$



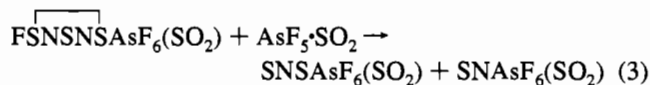
by the cycloaddition of SNSAsF_6 and SNAsF_6 , with little or no dissociation to FSNSNSAsF_6 and AsF_5 .

Although this cycloaddition is symmetry-allowed, when SNAsF_6 and SNSAsF_6 were dissolved in SO_2 the solution was shown by ^{14}N NMR to contain only SN^+ and SNS^+ , with no evidence of **1**, even at -20 °C. However, cooling the solution below -20 °C, or removing the solvent (at -20 °C) gave a white solid, identified by its IR and Raman spectra and X-ray crystallography as $1(\text{AsF}_6)_2$ (see below), with no trace of either SNAsF_6 or SNSAsF_6 . Replacing the solvent regenerated SN^+ and SNS^+ in solution and removing it gave $1(\text{AsF}_6)_2$ back again, establishing eq 1.

Infrared spectra of $1(\text{AsF}_6)_2$, taken as Nujol mulls, exhibited bands due to **1**, AsF_6^- ,³⁶ and FSNSNS^+ .^{5,14} FSNSNSAsF_6 was observed neither in Raman spectra nor in ^{14}N NMR spectra of redissolved material, and it seems reasonable to infer that a fluoride ion transfer from AsF_6^- to **1** (according to eq 2) was



induced by grinding, suggesting that crystalline $1(\text{AsF}_6)_2$ is thermodynamically unstable, but kinetically stable, with respect to FSNSNSAsF_6 and AsF_5 at low pressures. Consistently, heating $1(\text{AsF}_6)_2$ at 80 °C for 20 h under dynamic vacuum effected a substantial increase in the intensities of the FSNSNSAsF_6 bands in the IR, and the ^{14}N NMR of the solid redissolved in SO_2 consisted of ca. 20% FSNSNS^+ and 40% each of SN^+ and SNS^+ . It is interesting that in SO_2 solution the reverse of eq 2 is observed, and SNAsF_6 and SNSAsF_6 are given quantitatively (^{14}N NMR) with excess AsF_5 .

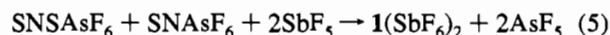


These findings differ from those of Padma and Mews,⁵ who reported that FSNSNSAsF_6 reacted quantitatively with excess AsF_5 at -30 °C to give a product that decomposed rapidly in SO_2 solution to SNAsF_6 and FSNSNSAsF_6 (vibrational spectroscopy), but appeared to be more stable in the solid state. The solid analyzed as $1(\text{AsF}_6)_2$, although its vibrational spectra were very different from those reported here.

Although good quantitative data are not available, it is well known that SbF_5 is a stronger Lewis acid than AsF_5 , and eq 4



should therefore be less energetically favorable than eq 2. Since SbF_5 is a syrupy liquid at room temperature, and AsF_5 is a gas, entropy effects will also be less significant. A sample of $1(\text{SbF}_6)_2$ was prepared as a colorless crystalline solid according to eq 5, and characterized by its Raman spectrum and X-ray



crystallography. Neither the appearance nor the Raman spectrum of the solid had changed after 12 months at -20 °C. By contrast, after 5 months under dry N_2 at -20 °C $1(\text{AsF}_6)_2$ had acquired a prominent red coloration on its surface probably

(34) Parsons, S.; Passmore, J.; Schriver, M. J.; White, P. S. *J. Chem. Soc., Chem. Commun.* **1991**, 369.

(35) Gimarc, B. M.; Warren, D. S. *Inorg. Chem.* **1991**, *30*, 3276.

(36) Begun, G. M.; Rutenberg, A. C. *Inorg. Chem.* **1967**, *6*, 2212.

(37) Rettig, S. J.; Trotter, J. *Acta Crystallogr.* **1987**, *43C*, 2260.

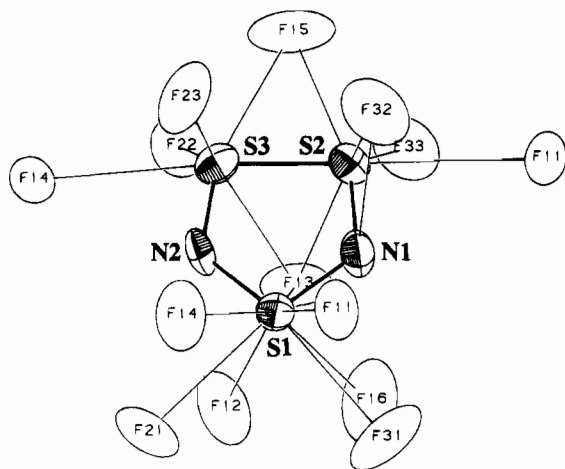
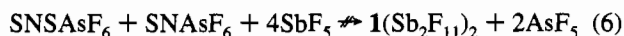


Figure 3. Structure of **1** showing anionic fluorine contacts.

attributable to $(S_3N_2^{+})_2$,^{3a,b} an attempt to obtain its Raman spectrum was unsuccessful. The crystal structure of $1(SbF_6)_2$ is disordered in the cations and the anions, although there is a prominent orthorhombic subcell.²⁵ An attempt to prepare $1(Sb_2F_{11})_2$ according to eq 6 gave only an oil, shown by Raman



spectroscopy to be a super-cooled liquid containing $SNSb_2F_{11}$ and $SNSSb_2F_{11}$. The reason for the instability of $1(Sb_2F_{11})_2$ is discussed below.

X-ray Crystal Structures of $1(MF_6)_2$ ($M = As, Sb$). The crystal structure of $1(AsF_6)_2$ is isomorphous with those of the selenium containing analogues $Se_xS_{3-x}N_2(AsF_6)_2$ ($x = 2, 3$),⁶⁻⁸

and contains $SNSNS^{2+}$ cations and three crystallographically independent, octahedral AsF_6^- anions, with significant contacts between cations and anions. The $SNSNS^{2+}$ cation (Figure 3) is planar, with maximum deviation from planarity 0.017(11) Å (N(1)). The contents of the unit cell are shown in Figure 4. The contents of the unit cell of $1(SbF_6)_2$, viewed along c , are included in Figure 5.

Bond distances and angles in **1** in both MF_6^- salts are very similar and presented in Table 5, and compared to analogous data for related compounds in Table 6. The data for $1(AsF_6)_2$ contains lower standard deviations and the structure is not disordered and therefore are used for purposes of comparison.

1 is most closely related to the 7π $SNSNS^{+}$ cation,³ from which it is formally derived by the removal of one electron; **1** is thus a 6π electron species, and this is confirmed at the 6-31G* level (see Figure 2). The lengths of the bonds S(2)–S(3) and N(1,2)–S(2,3) are significantly shorter than the corresponding bonds in $SNSNSAsF_6$,^{3b} whereas the lengths of S(1)–N(1,2) are not significantly different. This is consistent with the form of the SOMO of the $SNSNS^{+}$ cation (see Figure 2),^{3c} which is unoccupied in **1**. The antibonding interactions between S(2)–S(3) and N(1,2)–S(2,3) cause these bonds to shorten when this orbital is unoccupied, whereas there is little effect on S(1)–N(1,2) because S(1) lies on a node.

(38) (a) The order (b) of a bond X–Y, length D_b (Å), is given by

$$D_b = D_1 - 0.71 \log b$$

where D_1 is the sum of the covalent radii of X and Y (S 1.02, Se 1.17, N 0.73 Å). See ref 28b. (b) The S–N bond order is calculated by Nyburg's equation: $b(SN) = 0.429 + 6.85D_b - 3.825D_b^2$. See: Nyburg, S. C. *J. Cryst. Mol. Struct.* **1973**, *3*, 331.

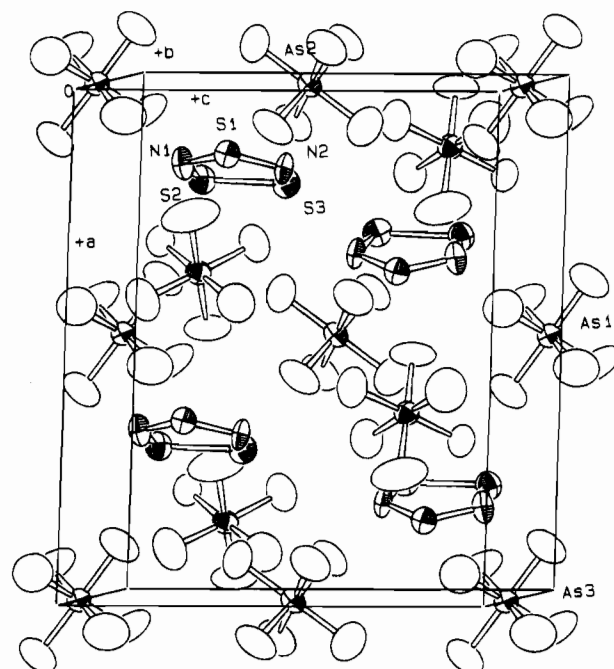


Figure 4. Unit cell of $1(AsF_6)_2$. Boundary ellipses are drawn at 50%.

Table 5. Bond Distances (Å) and Angles (deg) of **1** in $1(MF_6)_2$ ($M = As, Sb$)^a

	$1(AsF_6)_2$	$1(SbF_6)_2^b$
S(1)–N(1)	1.597(10)	1.59(1)
S(1)–N(2)	1.584(10)	1.59(1)
S(2)–S(3)	2.093(5)	2.08(1)
S(2)–N(1)	1.538(11)	1.53(1)
S(3)–N(2)	1.525(11)	1.53(1)
N(1)–S(1)–N(2)	101.1(5)	104.0(3)
S(3)–S(2)–N(1)	97.3(4)	98.2(2)
S(2)–S(3)–N(2)	96.3(4)	97.6(3)
S(1)–N(1)–S(2)	121.7(6)	119.4(3)
S(1)–N(2)–S(3)	123.5(6)	120.9(3)

^a MF_6^- bond distances and angles are included in the supplementary data. ^b Average distances and angles from the three equivalent rings.

Table 6. Comparison of the Geometry of **1** with Those of Similar Species

ref	this work	3b	41	6, 8 <i>a</i>	7 <i>b</i>
Ch(1)–N(1,2) ^c	1.591(7)	1.565(8)		1.694(14)	1.585(10)
N(1,2)–Ch(2,3)	1.532(8)	1.603(7)	1.568(3)	1.739(15)	1.70(1)
Ch(2)–Ch(2)	2.093(5)	2.143(5)	2.023(2)	2.334(3)	2.310(2)
∠Ch(1)	101.1(5)	107.0(5)		103.8(9)	107.5(5)
N(1,2)	122.6(4)	119.8(5)	116.2(3)	122.5(8)	122.0(4)
Ch(2,3)	96.8(3)	96.7(3)	95.1(1)	95.5(4)	94.2(2)

^a Sums of contact valencies:⁴⁸ Se(1) 0.74; Se(2,3) 0.60, 0.62. ^b Sums of contact valencies:⁴⁸ S(1) 0.43; Se(2,3) 0.62, 0.69. ^c Average values of chemically equivalent bonds; all AsF_6^- salts for $Se_xS_{3-x}N_2^{2+}$ ($x = 0-3$) cations.

A notable feature of the $SNSNS^{+}$ cation is its surprisingly long S–S bond length (2.143(5) Å),^{3b} and although S(2)–S(3) in **1** is 0.05 Å shorter (2.093(5) Å), it is still significantly longer than a formal S–S single bond (e.g. 2.055(2) Å in S_8).³⁷ The S–S bond in **1** consistently has a weak force constant (see below). The S–S bond order is calculated to be 0.84 by Pauling's equation,^{38a} which is lower than expected on the basis

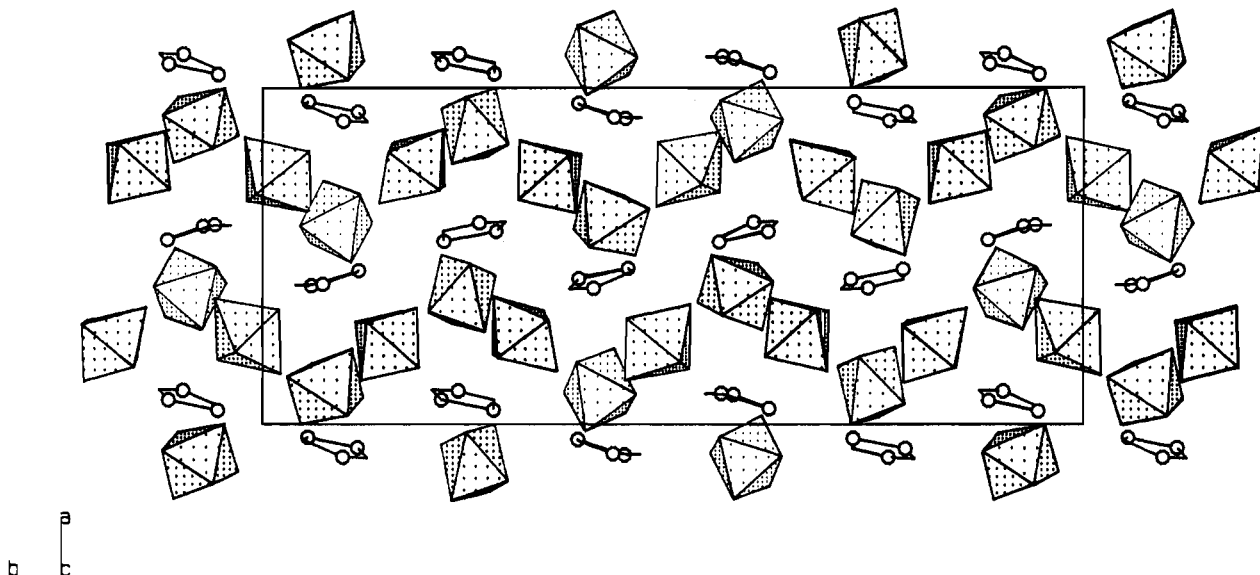


Figure 5. Contents of the unit cell of **1**(SbF₆)₂ viewed along *c*. A numbering diagram for the atoms with an ORTEP diagram have been deposited as supplementary material.

of the MO diagram shown in Figure 2, from which some S–S π bonding was anticipated. The weakness of the S–S bond in **1** also contrasts with the Se–Se bond lengths in the analogous $\overline{\text{SeNSeNSe}}^{2+}$ and $\overline{\text{SeNSNSe}}^{2+}$ cations (2.334(3) and 2.3097(15) Å, respectively)^{6–8} which possess bond orders of 1.02 and 1.10, respectively.^{38a} This relative weakening effect is also observed in other families of sulfur and selenium-containing cations (e.g. the chalcogen–chalcogen bond orders in S₄²⁺ and Se₄²⁺ are 1.09³⁹ and 1.21,⁴⁰ respectively; in PhCNChChN⁺, 1.06 (Ch = S) and 1.29 (Ch = Se);⁴¹ and in 1,5-dichalcogeniabicyclo-[3.3.0]ocatane dications, 0.76 (Ch = S)⁴² and 0.87 (Ch = Se)⁴³). The observation of this effect in CH₄²⁺ cations and the electronegativities of S and Se (2.58 and 2.55)⁴⁴ imply that it is unlikely to be due to gross molecular orbital differences,⁴⁵ and it may be associated with electrostatic repulsion across S–S bonds being more potent than across longer Se–Se bonds.

The average S(1)–N(1,2) (1.591(10) Å) and N(1,2)–S(2,3) (1.532(11) Å) bond lengths correspond to bond orders^{38b} of 1.65 and 1.95, respectively, and imply significant $3p\pi(\text{S})-2p\pi(\text{N})$ bonding, consistent with the simple π MO model shown in Figure 2. Banister⁴⁶ has shown that bond angles in SNS and NSN moieties are related to SN bond distance ($d(\text{SN})$ in pm) in unstrained systems by the following equations:

$$d(\text{SN}) = 213 - 0.4861\angle\text{S} \quad (\text{in NSN moieties})$$

$$d(\text{SN}) = 187.03 - 0.2263\angle\text{N} \quad (\text{in cationic SNS moieties})$$

The SN bond lengths in **1** correspond to ideal angles at S(1) and N(1,2) of 110.9 and 139.3°, respectively; since these are very different from the observed angles (101.5 and 122.6°); **1** likely experiences some ring strain which also appears to be reflected in the force constants (see below).

6-31G* calculations^{10,47} place the positive charge in **1** on the sulfur atoms (S(1) + 1.2; S(2,3) +0.86), consistent with the sums of the S–F contact valencies: S(1) 0.62, S(2) 0.5, and S(3) 0.5 vu.⁴⁸ In addition, cation–anion contacts are significantly stronger and more numerous than in SNSNSAsF₆ (in

which the sums of S–F contact valencies range from 0.21 to 0.24 vu),^{3b} consistent with the increased cationic charge. The pattern of the contacts (Figure 3) is consistent with the approximate C_{2v} symmetry of the cation, and identical to that

in the isomorphous crystal structure of $\overline{\text{SeNSeNSe}}(\text{AsF}_6)_2$,^{6,8} although as in other salts of S and Se containing cations (e.g. ChBr₃AsF₆; Ch = S, Se),⁴⁹ they are uniformly 0.10–0.12 vu weaker. With the exception of a weak N(1)–F(32) interaction (2.94(1) Å), there are no significant N–F contacts. This is also reflected in the crystal structures of all $(\text{Se}_x\text{S}_{3-x}\text{N}_2)_n(\text{AsF}_6)_2$ ($n = 1, 2$; $x = 0-3$), and is consistent with the weakness of NF bonding, and the calculated charge on N (–0.45). Analysis of the distribution of the S–F contacts in **1**(AsF₆)₂ based on simple VSEPR considerations⁵⁰ is likely complicated by the anisotropy of van der Waals radii⁵¹ and probably also by the effects of the total electron density distribution in **1**, as has been demonstrated by Gillespie and Bader, for example, in the crystal structure of S₄(AsF₆)₂·xSO₂ ($x = 0.6$).⁵²

The average As–F distances and F–As–F angles are 1.688(10) Å and 90.0(5)°, and not significantly different from the

- (39) Passmore, J.; Sutherland, G.; White, P. S. *J. Chem. Soc., Chem. Commun.* **1980**, 330.
 (40) Cardinal, G.; Gillespie, R. J.; Sawyer, J. F.; Vekris, J. E. *J. Chem. Soc., Dalton Trans.* **1982**, 765.
 (41) Belluz, P. D. B.; Cordes, A. W.; Kristof, E. M.; Kristof, P. V.; Liblong, S. W.; Oakley, R. T. *J. Am. Chem. Soc.* **1989**, *111*, 9276.
 (42) Iwasaki, F.; Toyoda, N.; Akaishi, R.; Fujihara, H.; Furukawa, N. *Bull. Chem. Soc. Jpn.* **1988**, *61*, 2563.
 (43) Iwasaki, F.; Morimoto, M.; Yasui, M.; Akaishi, R.; Fujihara, H.; Furukawa, N. *Acta Crystallogr.* **1991**, *47C*, 1463.
 (44) Huheey, J. E. *Inorganic Chemistry*, 3rd ed.; Harper and Row: New York, 1983.
 (45) Consistently, Laitinen has shown using minimal basis set *ab initio* calculations that there are no significant differences in the MO distributions for the series of all combinations in the series of molecules HS₂Se_{3-x}H ($x = 0-3$). Laitinen, R. 74th Canadian Chemical Conference and Exhibition, Hamilton, Ontario, Canada, 1991. Laitinen, R.; Pakkanen, T. *J. Mol. Struct. (THEOCHEM)* **1983**, *91*; **1985**, 124.
 (46) Banister, A. J.; Gorrell, I. B.; Roberts, R. S. *J. Chem. Soc., Faraday Trans. 2* **1985**, *81*, 1783.

- (47) Grein, F. *Can. J. Chem.* **1993**, *71*, 335.
 (48) Brown I. D. In *Structure and Bonding in Crystals*; O'Keeffe, M., Navrotsky, A., Eds.; Academic Press: London, 1981; Vol. 2. The bond valence for a S(IV)–F contact of length *R* is $(R/1.550)^{-3.8}$.
 (49) Johnson, J. P.; Murchie, M.; Passmore, J.; Tajik, M.; White, P. S.; Wong, C.-M. *Can. J. Chem.* **1987**, *65*, 2744.
 (50) Gillespie, R. J.; Hargittai, I. *The VSEPR Model of Molecular Geometry*; Allyn and Bacon: Boston, 1991. Sawyer, J. F.; Gillespie, R. J. *Prog. Inorg. Chem.* **1985**, *34*, 65.
 (51) Nyburg, S. C.; Faerman, C. H. *Acta Crystallogr.* **1985**, *41B*, 274.

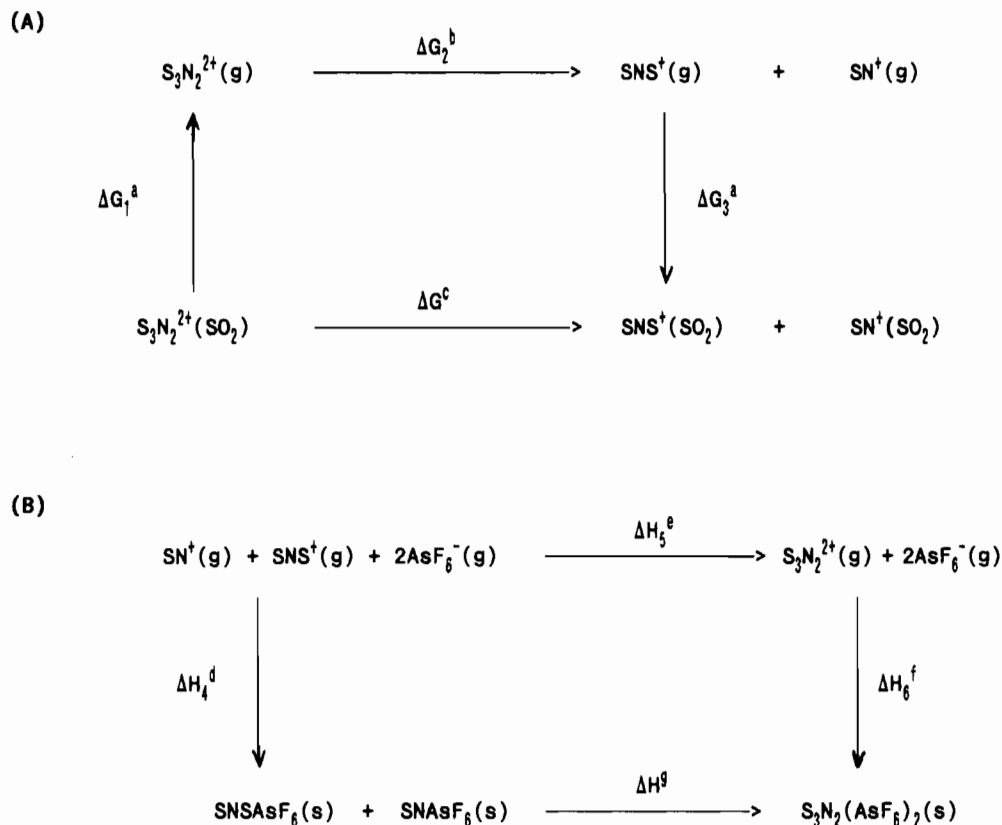


Figure 6. Thermochemical cycles for the estimation of ΔG for the dissociation of **1** in SO_2 (A) and ΔH for $\text{SNAsF}_6(\text{s}) + \text{SNSAsF}_6(\text{s}) \rightarrow \text{1}(\text{AsF}_6)_2(\text{s})$ (B). ^aFree energies of solvation ($\Delta G[\text{X}(\text{g}) \rightarrow \text{X}(\text{SO}_2)]$) were estimated using the Born equation:³⁰ $\Delta G_{\text{soln}} = \{(-Nz^2e^2/8\pi\epsilon_0r)[1 - (1/D)]\}$, where D is the dielectric constant of the solvent (15.4 for SO_2) and r is the rather vaguely defined as the radius of the ion (charge z). The molar volumes of SNSbF_6 (153.2 \AA^3),³³ SNSAsF_6 (167.1 \AA^3 ; see ref 58) and $\text{1}(\text{AsF}_6)_2$ (280.6 \AA^3) yield volumes⁵⁸ of SN^+ (38.2), SNS^+ (62.1) and **1** (70.6 \AA^3). The Born equation assumes ions to be spherical, which, although obviously a gross approximation in this case, implies radii (r) for SN^+ (2.09), SNS^+ (2.46) and **1** (2.56 \AA). Inserting these values into the Born equation gives ΔG_{soln} for SN^+ , SNS^+ and **1** as -311 , -264 and 1015 kJ mol^{-1} , respectively. Hence $\Delta G_1 = 1015$ and $\Delta G_3 = -575$ kJ mol^{-1} . We note that the shortcomings of the Born equation are well known,³⁰ although it has been used to rationalize trends in the solvation energies of related ions. ^b $\Delta G_2 = \Delta H_2 - T\Delta S_2$; $\Delta H_2 = -400$ kJ mol^{-1} . The molar entropy of a polyatomic species in the gas phase⁶⁹ is given by $S_m^\circ = 163 + 1.4M(2.6 \times 10^{-3})M^2$ and of diatomics by $S_m^\circ = 225 + 0.18M - 1004/M$, where M is the molecular weight. Hence S_m° for $\text{SN}^+(\text{g})$, $\text{SNS}^+(\text{g})$ and **1**(g) are 211, 256 and 297 $\text{J mol}^{-1} \text{ deg}^{-1}$, respectively, and $T\Delta S_2$ is 46 kJ mol^{-1} at 298 K. Hence $\Delta G_2 = -446$ kJ mol^{-1} . ^c $\Delta G = -6$ kJ mol^{-1} . ^d $\Delta H_4 = U[\text{SNAsF}_6] + U[\text{SNSAsF}_6] = 1065$ kJ mol^{-1} . ^e $\Delta H_5 = +400$ kJ mol^{-1} . ^f $\Delta H_6 = U[\text{1}(\text{AsF}_6)] = 1493$ kJ mol^{-1} . ^g $\Delta H_5 = -28$ kJ mol^{-1} .

corresponding values in KAsF_6 (1.719(3) \AA and 90.0(2) $^\circ$).⁵³ There is significant deviation in the As(1)–F bond lengths from ideal octahedral geometry, and this can be largely related to the strengths of the contacts made by a particular fluorine atom. The sums of the fluorine contact bond valencies (ν) versus As(1)–F bond length (\AA) (in decreasing order) are as follows: F15, 0.26 and 1.737(10); F14, 0.17 and 1.697(9); F13, 0.21 and 1.685(9); F16, 0.07 and 1.678(12); F11, 0.15 and 1.674(9); F12, 0.07 and 1.669(11) \AA . Thus, overall, the stronger the contacts, the longer the As–F bond. The total strengths of the contacts made by the fluorine atoms in anions **2** and **3** are all 0.10–0.13 ν , and consistently there is no significant As–F bond length distortion in these anions. The six independent SbF_6^- anions in **1**(SbF_6) have bond distances and angles in the expected range.

Thermodynamic Instability of SNSNS^{2+} in the Gas Phase and in Solution and Its Stabilization as the MF_6^- Salts in the Solid State by Crystal Lattice Energy. Although the cycloaddition of SN^+ to SNS^+ to give **1** is allowed by symmetry, the total energies (6-31G**/6-31G*)⁵⁴ of these cations show that this reaction is endothermic by 400 kJ mol^{-1} in the gas

phase.^{10,47,54} Reference to a thermochemical cycle suggests that this is due to the electrostatic repulsion of the two monocations (estimated to be between ca. 460 and 695 kJ mol^{-1} for an approach distance of 2–3 \AA) overcoming the exothermic bond reorganization associated with the cycloaddition (estimated to be worth ca. -190 kJ mol^{-1}).⁵⁵ By contrast, the corresponding dissociation of the related monocationic SNSNS^{2+} to $\text{SN}^+ + \text{SNS}^+$ or $\text{SN}^+ + \text{SNS}^*$ was recently shown by Gimarc

(54) The following results were obtained at the 6-31G**/6-31G* level (see refs 10 and 47). **1**: S(1)–N(1,2) 1.596 \AA , N(1,2)–S(2,3) 1.535, S(2)–S(3) 2.092, $\angle\text{NSN}$ 98.84 $^\circ$, $\angle\text{SNS}$ 124.34, $\angle\text{NSS}$ 96.24. Total energy: -1300.50403 hartrees. SNS^+ : S–N 1.474, $\angle\text{SNS}$ 180. Total energy: -849.09024 hartrees. SN^+ : S–N 1.397. Total energy: -451.56553 hartrees. 1 hartree = 2622 kJ mol^{-1} .

(55) An order of magnitude for $\Delta H[\text{SN}^+(\text{g}) + \text{SNS}^+(\text{g}) \rightarrow \text{1}(\text{g})]$ can be obtained from $\Delta H_{\text{electrostatic}}[\text{SN}^+ + \text{SNS}^+] + 2\text{BET}[\text{SN}]\text{SN}^+ + \text{BET}[\text{SN}]\text{SN}^+ - 2\text{BET}[\text{S}(1)–\text{N}(1,2)]_1 - 2\text{BET}[\text{N}(1,2)–\text{S}(2,3)]_1 - \text{BET}[\text{S}(2)–\text{S}(3)]_1$ (BET \equiv Bond Enthalpy Term). $\Delta H_{\text{repulsion}}[\text{SN}^+ + \text{SNS}^+]$ is the electrostatic repulsion associated with bringing SN^+ and SNS^+ together and assuming a point charge model. Between 2 and 3 \AA this is $463 < \Delta H_{\text{repulsion}} < 695$ kJ mol^{-1} . $\text{BET}[\text{SN}]\text{SN}^+$ is the SN bond dissociation energy in SNS^+ , 473 kJ mol^{-1} .⁶⁸ $\text{BET}[\text{S}(1)–\text{N}(1,2)]_1$ (343 kJ mol^{-1}) and $\text{BET}[\text{N}(1,2)–\text{S}(2,3)]_1$ (410 kJ mol^{-1}) were obtained from the linear correlation of $\text{BET}[\text{SN}]$ with SN bond length.⁶⁸ $\text{BET}[\text{S}(2)–\text{S}(3)]_1$ was estimated to be 200 kJ mol^{-1} by comparison with $\text{BET}[\text{SS}]_3$ (226 kJ mol^{-1}). $\text{BET}[\text{SN}]\text{SN}^+$ has been determined experimentally to be 511 kJ mol^{-1} (O'Hare, P. A. G. *J. Chem. Phys.* 1970, 52, 2992). Hence $\Delta H[\text{SN}^+(\text{g}) + \text{SNS}^+(\text{g}) \rightarrow \text{1}(\text{g})]$ is estimated to be between about 170 and 400 kJ mol^{-1} .

(52) Bader, F. W.; Gillespie, R. J.; MacDougall, P. J. In *Molecular Structure and Energetics: From Atoms to Polymers, Isoelectronic Analogies*; Liebman, J. F., Greenberg, A., Eds.; VCH: New York, 1989; p 1.

(53) Gafner, G.; Kruger, G. *J. Acta Crystallogr.* 1974, 30B, 250.

and Warren on the basis of *ab initio* SCF MO calculations to be both symmetry- and thermodynamically-forbidden,³⁵ in agreement with its indefinite stability in solution and in the solid state.

An estimate of the thermodynamic instability of **1** in SO₂ solution may be made by reference to the free energy cycle shown in Figure 6a, which indicates that it dissociates in solution ($\Delta G[\mathbf{1}(\text{SO}_2) \rightarrow \text{SN}^+(\text{SO}_2) + \text{SNS}^+(\text{SO}_2)] \approx -6 \text{ kJ mol}^{-1}$) because although the solvation of a dication is favored over two monocations, this is not sufficient to overcome the electrostatic repulsion between SN⁺ and SNS⁺ associated with the gas phase dissociation enthalpy. Although these data are in no sense quantitative, the modest instability of **1** with respect to SNS⁺ and SN⁺ is consistent with the observed stability of the related Se-containing cations, Se_{3-x}S_xN₂²⁺ (x = 0–2) in solution. This can be associated with the tendency of Se to form extended or polymeric structures where the sulfur analogues are discrete monomers (e.g. SO₂ and (SeO₂)_x; OSF₄ and (OSeF₄)_x)^{56a,b} resulting in a less positive gas phase enthalpy of dissociation of the selenium containing dications. This enthalpy term contains a $\pi \rightarrow \sigma$ bond energy term that is more favorable for selenium, and an electrostatic term that is less unfavorable for the larger selenium (relative to sulfur) containing dications.

The stability of **1**(AsF₆)₂ in the solid state can be understood in terms of the thermochemical cycle shown in Figure 6b. By using the calculated lattice energies of **1**(AsF₆)₂ and SNSAsF₆, and the estimated value of $U[\text{SNAsF}_6]$ (556 kJ mol⁻¹) with the value of $\Delta H[\text{SN}^+(\text{g}) + \text{SNS}^+(\text{g}) \rightarrow \mathbf{1}(\text{g})]$ obtained at the 6-31G* level (400 kJ mol⁻¹) [415.5 kJ mol⁻¹ at the 3-21G* level],^{10,54} we deduce that **1**(AsF₆)₂(s) is 28 kJ mol⁻¹ more stable than a mixture of SNAsF₆(s) and SNSAsF₆(s). In fact **1**(g) represents a local potential energy minimum, with a barrier to dissociation (3-21G*/3-21G*) of ca. 45 kJ mol⁻¹.⁴⁷ The high lattice energy of the 1:2 salt (1493 kJ mol⁻¹) compared to those of two 1:1 salts (SNAsF₆, 556; SNSAsF₆, 509 kJ mol⁻¹) forces the system into the local **1** minimum. The molar entropies of SNAsF₆(s), SNSAsF₆(s) and **1**(AsF₆)₂(s) are estimated by the method of Latimer^{56b} to be 282, 318 and 600 J mol⁻¹ deg⁻¹, respectively, implying that $\Delta S[\text{SNSAsF}_6(\text{s}) + \text{SNAsF}_6(\text{s}) \rightarrow \mathbf{1}(\text{AsF}_6)_2(\text{s})]$ is zero, or very small. The existence of **1**(MF₆)₂(s) are therefore attributable to the high lattice energy of 1:2 salts. Similar factors are responsible for the stability of S₂I₄(AsF₆)₂ + I₂ over 2SI₃AsF₆,⁵⁷ and the instability of salts containing monovalent group 2 elements, e.g. CaF with respect to Ca and CaF₂. To our knowledge this is the first example of a crystal-lattice-enforced cycloaddition reaction.

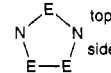
The calculated (6-31G*) geometry of **1**(g)⁵⁴ is remarkably similar to that observed in the solid state. This is because lattice energies are rather insensitive to small changes in the size of large ions,^{30,56b} so that the lattice energy contribution to the total solid state potential energy function is rather flat, and the gas phase equilibrium geometry of **1** is preserved on its incorporation into the crystal lattice, with the result that the crystal structure of **1** shows no abnormal features attributable to partial dissociation into SNS⁺ and SN⁺.

Normal coordinate analyses of **1**, SeNSeNSe²⁺ and SeNSNSe²⁺ were performed with the aim of establishing whether the gas phase instability of **1** correlates with the shape

Table 7. Bond Distances, Orders, and Force Constants

bond	species	dist, Å	order ^d	force const, ^b		
				N m ⁻¹	ref	
N–S	HSNO	1.70	1.0	179	61	
	CISNSCI ⁺	1.582	1.95	620	62	
	HNSO	1.51	2.0	647	61	
	NS	1.494	2.1	852	63	
	SNS ⁺	1.463	2.2	827	62	
	SN ⁺	1.440	2.4	1149	63	
	SeNSNSe ²⁺	top ^c	1.591	1.6	333	
		side	1.532	1.95	443	
N–Se	SeNSNSe ²⁺	1.584	1.7	339	68	
	NSe	1.652	2.3	640	63	
	SeNSNSe ²⁺	1.696	2.0	425	7	
	SeNSeNSe ²⁺	top ^c	1.694	2.0	375	6, 8
		side	1.739	1.7	304	
S–S	S ₂	1.889	1.6	496	63	
	S ₂ Cl ₂	1.97	1.3	243	64	
	S ₂ Br ₂	1.98	1.3	253		
	H ₂ S ₂	2.055	1.0	256	65	
	SNSNS ²⁺	2.093	0.8	155		
Se–Se	Se ₂	2.166	1.8	350	63	
	Se ₂ Cl ₂	2.32	1.1	198	64	
	Se ₂ Br ₂	2.32	1.1	193	64	
	SeNSNSe ²⁺	2.310 ^d	1.1	197 ^d	7	
	SeNSeNSe ²⁺	2.334 ^d	1.0	222 ^d	6, 8	

^a See ref 38. ^b All force constants calculated with our procedures and programs from geometry and frequencies in the references cited. ^c "Top" and "side" refer to



^d Note that the longer of these bonds is found to have the stronger force constant. The two bonds are in different molecules, and therefore, the puzzling result may be due to differing ring geometries and strain.

of the potential energy surface in the solid state. Bond lengths, bond orders, and the corresponding force constants are listed in Table 7 with data of related species for comparison. All calculations used the Wilson F and G matrix method²⁶ and a least squares fitting procedure to determine the force constants; all force constants in Table 7 were calculated with the same programs. The bond length, force constant relations agree well with Badger's rule;²⁷ but by comparison with various non-cyclic species the N–S and N–Se force constants are consistently smaller by about 25%. Thus the N–S distance in SeNSNSe²⁺ of 1.532 Å goes with a force constant of 443 N m⁻¹ compared to more than 600 N m⁻¹ for acyclic N–S bonds of similar length, and it is possible that this is associated with ring strain (see above) and/or (likely more importantly) the effect of the intracationic electrostatic repulsions. The N–Se bonds seem to show the same pattern, but there are fewer data for comparison. Equivalent S–N and/or Se–N bonds in **1** and SeNSNSe²⁺ possess similar stretching force constants, and although different trends are apparent in the stretching constants in SeNSeNSe²⁺, this is likely due to the different pattern of Se–N bond lengths (Se(1)–N(1,2) < Se(2,3)–N(1,2); see Table 6).^{6,8} The S–S force constant is weaker than in the non-cyclic examples while the Se–Se bonds have relatively strong single bond force constants, which is consistent with the observed bond lengths in these cations (see above). The calculation⁴⁷ of electron density in **1** shows strong positive charges on the two adjacent S atoms (see above). The electrostatic repulsion will lengthen and weaken the S–S bond and the attraction of nearby anions will add to the effect. The Se–Se bonds should show

(56) (a) Wells, A. F. *Structural Inorganic Chemistry*, 5th ed.; Oxford University Press: Oxford U.K., 1984. (b) Johnson, D. A. *Some Thermodynamic Aspects of Inorganic Chemistry*, 2nd ed.; Cambridge University Press: Cambridge, U.K., 1982.

(57) Murchie, M. P.; Johnson, J. P.; Passmore, J.; Sutherland, G. W.; Tajik, M.; Whidden, T. K.; White, P. S.; Grein, F. *Inorg. Chem.* **1992**, *31*, 273.

this to a smaller degree since the atoms are farther apart both within the cation and between ions.

The stability of a salt of **1** depends critically upon its lattice energy, and hence upon the size of the counteranion (the larger the counteranion, the smaller the lattice energy). Estimates based on the equations of Bartlett and Kapustinskii⁵⁸ imply that while $\mathbf{1}(\text{AsF}_6)_2$ and $\mathbf{1}(\text{SbF}_6)_2$ possess similar stabilities, the significantly larger size of the $\text{Sb}_2\text{F}_{11}^-$ anion makes $\mathbf{1}(\text{Sb}_2\text{F}_{11})_2$ unstable with respect to $\text{SNSb}_2\text{F}_{11}$ and $\text{SNSb}_2\text{F}_{11}$. This is reflected in our unsuccessful attempt to obtain $\mathbf{1}(\text{Sb}_2\text{F}_{11})_2$ according to eq 6, from which an oil containing only SN^+ , SNS^+ and $\text{Sb}_2\text{F}_{11}^-$ was obtained.

The instability of $\mathbf{1}(\text{AsF}_6)_2(\text{s})$ with respect to $\text{FSNSNSAsF}_6(\text{s})$ and $\text{AsF}_5(\text{g})$ (eq 2) can be contrasted with the fluoride ion abstraction reaction of FSNSNS^+ and AsF_5 in SO_2 established by ^{14}N NMR (eq 3). Simple thermochemical estimates⁵⁹ show that although $\Delta H[\text{eq 2}] < +24 \text{ kJ mol}^{-1}$, the thermodynamic instability of $\mathbf{1}(\text{AsF}_6)_2$ with respect to FSNSNSAsF_6 is associated with the large molar entropy of gaseous AsF_5 ($\Delta G[\text{eq 2}] < -15 \text{ kJ mol}^{-1}$). In addition, eq 2 will be displaced to the right at low pressures by the law of mass action. In SO_2 solution SNS^+ and SN^+ possess increased stability with respect to **1** (see above), and AsF_5 is complexed with the solvent,⁶⁰ making entropy less important. Equation 3 therefore proceeds quantitatively in solution to give SN^+ and SNS^+ , via **1**. By contrast, the stability of $\mathbf{1}(\text{SbF}_6)_2(\text{s})$ relative to $\mathbf{1}(\text{AsF}_6)_2(\text{s})$ is due to the comparatively low molar entropy of SbF_5 , which is a viscous, syrupy liquid at room temperature.

(58) If the radii of A^+ and A^{2+} in A^+B^- and $\text{A}^{2+}\text{B}^{2-}$ can be considered to be equal, then by the Kapustinskii equation, the lattice energy of AB_2 , $U[\text{AB}_2]$, is 3 times the lattice energy of AB ($U[\text{AB}]$). $U[\text{AB}]$ can be estimated from the molar volume of AB ($V[\text{AB}]$) by Bartlett's equation:^{31,66}

$$U[\text{AB}] = 2336.5 V[\text{AB}]^{-1/3} + 110.5$$

Applying this approach to $\mathbf{1}(\text{AsF}_6)_2$, $U[\mathbf{1}(\text{AsF}_6)_2] = 1583.2 \text{ kJ mol}^{-1}$ is obtained using $V[\mathbf{1}(\text{AsF}_6)_2] = 280.6 \text{ \AA}^3$ and $V[\text{AsF}_6^-] = 105 \text{ \AA}^3$.⁶⁶ This compares to 1493 kJ mol^{-1} obtained by extended calculation, and so a factor of 0.94 was applied to estimates of $U[\mathbf{1}(\text{SbF}_6)_2]$ and $U[\mathbf{1}(\text{Sb}_2\text{F}_{11})_2]$. Using $V[\text{A}^+\text{SbF}_6^-] = V[\text{A}^+\text{AsF}_6^-] + 1032$ and $V[\text{A}^+\text{Sb}_2\text{F}_{11}^-] = V[\text{A}^+\text{SbF}_6^-] + \{V[\text{SNSb}_2\text{F}_{11}] - V[\text{SNSbF}_6]\} = V[\text{A}^+\text{SbF}_6^-] + 9633$ gives $U[\mathbf{1}(\text{SbF}_6)_2] = 1467$ and $U[\mathbf{1}(\text{Sb}_2\text{F}_{11})_2] = 1317 \text{ kJ mol}^{-1}$. The lattice energy of SNSbF_6 determined by extended calculation to be $541.3 \text{ kJ mol}^{-1}$ agrees well with the value obtained from Bartlett's equation (547), which gives $U[\text{SNSb}_2\text{F}_{11}] = 481.7 \text{ kJ mol}^{-1}$ (using $V[\text{SNSb}_2\text{F}_{11}] = 249.3 \text{ \AA}^3$).³³ $U[\text{SNSbF}_6]$ was estimated to be $501.3 \text{ kJ mol}^{-1}$, using a molar volume of 177.1 \AA^3 (see: Johnson, J. P.; Passmore, J.; White, P. S.; Banister, A. J.; Kendrick, A. G. *Acta Crystallogr.* **1987**, *43C*, 1651), and assuming the same deviation from Bartlett's equation as determined for SNSAsF_6 by extended calculation ($-25.3 \text{ kJ mol}^{-1}$). Similarly $U[\text{SNSb}_2\text{F}_{11}] = 445.3 \text{ kJ mol}^{-1}$ using a molar volume of 273.2 \AA^3 . Hence by the methods of Figure 4b, $\Delta H[\text{SNS}^+\text{X}^- + \text{SN}^+\text{X}^- \rightarrow \mathbf{1}(\text{X}^-)_2]$ is -24 kJ mol^{-1} for $\text{X} = \text{SbF}_6^-$ and $+10 \text{ kJ mol}^{-1}$ for $\text{X} = \text{Sb}_2\text{F}_{11}^-$. Alternatively, the lattice energies of $\mathbf{1}(\text{AsF}_6)_2$ can be estimated directly from the Kapustinskii equation^{56b} in the form

$$U = \frac{1.214 \times 10^5 v z^+ z^-}{r[\mathbf{1}] + r[\text{AsF}_6^-]} \left(1 - \frac{34.5}{r[\mathbf{1}] + r[\text{AsF}_6^-]} \right) [\text{kJ/mol}]$$

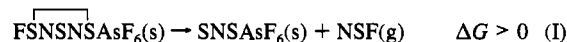
using $r[\text{AsF}_6^-] = 293 \text{ pm}$ and $r[\mathbf{1}] = 256 \text{ pm}$ and as $z^+ = 2$ and $z^- = 1$, then $U[\mathbf{1}(\text{AsF}_6)_2] = 1243 \text{ kJ mol}^{-1}$. Comparing this to the value obtained from the extended calculation (1493 kJ mol^{-1}) implies a "calibration factor" of 1.20. Applying this method to the lattice energies of $\mathbf{1}(\text{SbF}_6)_2$ and $\mathbf{1}(\text{Sb}_2\text{F}_{11})_2$ gives values of 1471 and 1322 kJ mol^{-1} , respectively, leading to values of $\Delta H[\text{SNS}^+\text{X}^- + \text{SN}^+\text{X}^- \rightarrow \mathbf{1}(\text{X}^-)_2]$ = -29 kJ mol^{-1} ($\text{X} = \text{SbF}_6^-$) and $+6 \text{ kJ mol}^{-1}$ ($\text{X} = \text{Sb}_2\text{F}_{11}^-$). While these methods of estimation are crude, it is likely that $\mathbf{1}(\text{Sb}_2\text{F}_{11})_2$ is 20 – 50 kJ mol^{-1} less stable than $\mathbf{1}(\text{AsF}_6)_2$ with respect to dissociation to the 1:1 salts.

Conclusion

We have shown that $\mathbf{1}(\text{AsF}_6)_2$, which contains the SNSNS^{2+} cation, long of theoretical interest because of its 6π electron configuration, may be prepared by the lattice enforced cycloaddition of SNAsF_6 and SNSAsF_6 on formation of solid $\mathbf{1}(\text{AsF}_6)_2$. However, the instability of **1** with respect to SNS^+ and SN^+ in solution is anomalous in terms of the stabilities of its selenium containing analogs, $\text{Se}_x\text{S}_{3-x}\text{N}_2^{2+}$ ($x = 1$ – 3) which retain their ring structures in solution, and the stabilities of other sulfur–nitrogen containing "electron rich aromatics".

High level MO calculations show that **1** is indeed unstable (by 400 kJ mol^{-1}) with respect to SN^+ and SNS^+ in the gas phase, although it resides in a shallow local potential energy minimum (activation barrier to dissociation ca. 45 kJ mol^{-1}). The similarity between the calculated bond distances for gas phase SNSNS^{2+} and those observed in solid $\mathbf{1}(\text{AsF}_6)_2$ implies that the potential energy surface of SNSNS^{2+} is dominated by the gas phase component. Simple estimates of the solution thermochemistry suggest that **1** is only marginally unstable ($\Delta G_{\text{dissoc}} = -6 \text{ kJ mol}^{-1}$) in SO_2 , because $\Delta G_{\text{sol}}[\mathbf{1}]$ is not large

(59) The thermochemistry of eq 2 can be assessed as follows: using $\Delta H_f[\text{SNSAsF}_6(\text{s})] = -1413 \text{ kJ mol}^{-1}$,⁶⁷ $\Delta H_f[\text{SNAsF}_6(\text{s})] = -1300 \text{ kJ mol}^{-1}$,⁶⁸ and $\Delta H[\text{Figure 4b}] = -28 \text{ kJ mol}^{-1}$, $\Delta H_f[\mathbf{1}(\text{AsF}_6)_2(\text{s})]$ is calculated to be $-2744 \text{ kJ mol}^{-1}$. FSNSNSAsF_6 can be prepared from the cycloaddition reaction of SNSAsF_6 and NSF in SO_2 and isolated as a stable solid.^{5,14} Assuming that the stability of $\text{FSNSNSAsF}_6(\text{s})$ is a thermodynamic, rather than a kinetic, effect



$\Delta S[\text{eq I}]$ can be estimated to be $+154 \text{ J mol}^{-1} \text{ deg}^{-1}$, so that at 298 K

$$\Delta H[\text{eq I}] > 46 \text{ kJ mol}^{-1}$$

Substituting $\Delta H_f[\text{SNSAsF}_6] = -1413$ and $\Delta H_f[\text{NSF}] = -20.9 \text{ kJ mol}^{-1}$ ⁷⁰ gives

$$\Delta H_f[\text{FSNSNSAsF}_6] < -1480 \text{ kJ mol}^{-1}$$

$\Delta H_f[\text{AsF}_5] = -1237 \text{ kJ mol}^{-1}$ ⁷¹ gives

$$\Delta H[\text{eq 2}] < +24 \text{ kJ mol}^{-1}$$

Estimating the S° for $\mathbf{1}(\text{AsF}_6)_2(\text{s})$, $\text{FSNSNSAsF}_6(\text{s})$ and AsF_5 to be 600 , 407 and $325 \text{ kJ mol}^{-1} \text{ deg}^{-1}$,⁷² respectively, gives at 298 K

$$\Delta G[\text{eq 2}] < -15 \text{ kJ mol}^{-1}$$

- (60) Brownstein, M.; Gillespie, R. J. *J. Am. Chem. Soc.* **1970**, *92*, 2718.
Chen, G. S. H.; Passmore, J. *J. Chem. Soc., Dalton Trans.* **1979**, 1257.
(61) Tchir, P. O.; Spratley, R. D. *Can. J. Chem.* **1975**, *53*, 2311, 2318.
(62) Schnepel, F.-M. *Spectrochim. Acta* **1980**, *36A*, 895.
(63) Huber, K. P.; Herzberg, G. *Constants of Diatomic Molecules*; Van Nostrand Reinhold: New York, 1979.
(64) Winnewisser, G.; Winnewisser, M.; Gordy, W. *J. Chem. Phys.* **1968**, *49*, 3465.
(65) Zengin, N.; Giguère, P. A. *Can. J. Chem.* **1959**, *37*, 632.
(66) Richardson, T. J.; Tanzella, F. L.; Bartlett, N. *J. Am. Chem. Soc.* **1986**, *108*, 4937.
(67) O'Hare, P. A. G.; Awere, E. G.; Parsons, S.; Passmore, J. *J. Chem. Thermodyn.* **1989**, *21*, 153.
(68) Parsons, S.; Passmore, J. *Inorg. Chem.* **1992**, *31*, 526.
(69) $S_m^\circ[\text{FSNSNSAsF}_6]$ and $S_m^\circ[\text{SNSAsF}_6]$ were estimated to be 407 and $318 \text{ kJ mol}^{-1} \text{ deg}^{-1}$ by the method of Latimer.^{56b} $S_m^\circ[\text{NSF}]$ is given by the methods outlined in footnote b, Figure 6, to be $243 \text{ J mol}^{-1} \text{ deg}^{-1}$. At 298 K $\text{TAS}[\text{eq I}] = +46 \text{ kJ mol}^{-1}$.
(70) Larson, J. W.; Johnson, G. K.; O'Hare, P. A. G.; Hubbard, W. N.; Glemser, O. *J. Chem. Thermodyn.* **1973**, *5*, 689.
(71) O'Hare, P. A. G. *J. Chem. Thermodyn.* **1993**, *25*, 391.
(72) S_m° for FSNSNSAsF_6 and $\mathbf{1}(\text{AsF}_6)_2$ were obtained by Latimer's method (ref 56b), for AsF_5 by the methods of Figure 6, footnote b.

enough to overcome the gas phase dissociation energy. The well known preference of Se for extended σ -bonded structures acts to reduce the gas phase dissociation energy for all $\text{Se}_x\text{S}_{3-x}\text{N}_2^{2+}$, enabling these cations to be stable in solution. The similarity of all $\text{Se}_x\text{S}_{3-x}\text{N}_2^{2+}$ is supported by a normal coordinate analysis of their vibrational spectra (for $x = 0, 2, 3$), which shows that a consistent set of force constants characterize their force fields.

In the solid state $\mathbf{1}(\text{AsF}_6)_2$ is stabilized by its high lattice energy, and the stability of other salts depends critically on this parameter. Thus SNSNS^{2+} can be said to be "lattice stabilized". Replacement of AsF_6^- with a larger counteranion was expected to decrease the lattice energy and therefore the stability of the resulting salt, and although we were able to prepare the slightly larger $\mathbf{1}(\text{SbF}_6)_2$, an attempt to obtain $\mathbf{1}(\text{Sb}_2\text{F}_{11})_2$ led only to a mixture of $\text{SNSb}_2\text{F}_{11}$ and $\text{SNSb}_2\text{F}_{11}$. It is clear that the symmetry-allowed cycloaddition of SNS^+ and SN^+ will not occur without the stabilizing influence of the crystal lattice, and to our knowledge, this is the first example of a "lattice-enforced" cycloaddition reaction. We recently showed that both S_8^{2+} ⁷³ and S_4^{2+} ^{74,75} are also lattice stabilized in $\text{S}_8(\text{AsF}_6)_2$ and $\text{S}_4(\text{AsF}_6)_2 \cdot \text{AsF}_3$, respectively. Interestingly, the cycloaddition of 2S_2^{*+} to S_4^{2+} is symmetry disallowed;⁷⁶ therefore, if S_4^{2+} is formed via 2S_2^{*+} , the cycloaddition is a lattice-enforced disallowed cycloaddition. Many dianions are unstable in the gas phase to loss of an electron (e.g. O^{2-} , CO_3^{2-} , SO_4^{2-})⁷⁷ and are therefore lattice stabilized in the solid state and stabilized by solvation energy in solution.

Acknowledgment. We thank Drs. A. G. Kendrick and A. J. Banister (both of Durham University)⁷⁸ and A. W. Apblett⁷⁹ for their preliminary results in this project, Dr. E. G. Awere for technical assistance, Dr. G. Schatte for obtaining FT-Raman spectra, Prof. N. Bartlett for a program to calculate U_{elec} terms in lattice energy determinations, Dr. F. Grein for his interest in this problem and for the results of *ab initio* calculations on $\mathbf{1}$ prior to publication and the calculation of its vibrational frequencies, and Dr. B. Vincent of Molecular Corp. for collecting the data on the rotating anode generator. Funding in the form of operating grants from the NSERC (Canada) and graduate fellowships from the NSERC (M.J.S.) and the Canadian Commonwealth Scholarship and Fellowship Committee (S.P.) is gratefully acknowledged.

Supplementary Material Available: Table S1, containing details of the lattice energy determinations of SNSAsF_6 , SNSbF_6 , and $\mathbf{1}(\text{AsF}_6)_2$, Tables S2–5, giving more complete crystal data, anisotropic thermal parameters, extended bond distances and valences, and extended bond and contact angles for $\mathbf{1}(\text{AsF}_6)_2$, Table S6, listing assignments for the FT Raman spectrum of " $\mathbf{1}(\text{Sb}_2\text{F}_{11})_2$ ", Table S7, giving force constants for $\mathbf{1}$, $\text{Se}_3\text{N}_2^{2+}$, and $\text{Se}_2\text{SN}_2^{2+}$, and Tables S8–10, containing more complete crystal data, anisotropic temperature factors, and extended table of bond distances and angles for $\mathbf{1}(\text{SbF}_6)_2$, as well as Figures S1–4, displaying the Raman spectra of $\mathbf{1}(\text{SbF}_6)_2$ and " $\mathbf{1}(\text{Sb}_2\text{F}_{11})_2$ ", the structure of the SeNSeNSe^{2+} cation in $\text{Se}_3\text{N}_2(\text{AsF}_6)_2$, showing anionic contacts in the same orientation as Figure 3 in the main paper, intended to illustrate its isomorphous relationship to $\mathbf{1}(\text{AsF}_6)_2$, and the asymmetric unit of $\mathbf{1}(\text{SbF}_6)_2$ viewed along c (this portion is at the extreme left end of the cell as shown in Figure 5) (33 pages). Ordering information is given on any current masthead page.

- (73) Tomaszkiwicz, I.; Passmore, J.; Schatte, G.; Sutherland, G. W.; O'Hare, P. A. G. *J. Chem. Thermodyn.* **1994**, *26*, 299.
 (74) Cameron, T. S.; Dionne, I.; Grein, F.; Parsons, S.; Passmore, J.; Sannigrahi, M. Presented at the Winter Fluorine Chemistry Conference, St. Petersburg, FL, Jan 1993; Abstract P29.
 (75) Dionne, I. M.Sc. Thesis, Department of Chemistry, University of New Brunswick, Fredericton, NB, Canada, 1993.
 (76) Sannigrahi, M.; Grein, F. *Can. J. Chem.* **1994**, *72*, 298.

- (77) From *ab initio* calculations: Janoschek. *R. Z. Anorg. Allg. Chem.* **1992**, *616*, 101.
 (78) Kendrick, A. G. Ph.D. Thesis, Durham University, Durham, England, 1986.
 (79) Apblett, A. W. B.Sc. Hons. Thesis, Department of Chemistry, University of New Brunswick, Fredericton, NB, Canada, 1984.